Numerical Eulerian method for linearized gas dynamics in the high frequency regime

Y. Noumir[†,✉1], F. Dubois[‡], ✉2, O. Lafitte [†,*,,✉3]

[†]LAGA, Institut Galilée, Université Paris 13, Villetaneuse.
[‡] Conservatoire National des Arts et Métiers, Paris.
*CEA DEN DM2S, Centre de Saclay, Gif sur Yvette.

✉1 nyouness@math.univ-paris13.fr
✉2 francois.dubois@cnam.fr
✉3 lafitte@math.univ-paris13.fr

December 22, 2011

Abstract

We study the propagation of an acoustic wave in a moving fluid in the high frequency regime. We calculate a high-frequency approximation of the solution of this problem using an Eulerian method.

The model retained is a linearized Euler system around a mean fluid flow. For any regular mean flow, we derive a conservative transport equation for the geometrical optics approximation. We introduce the *stretching matrix* corresponding to this system, from which we deduce the geometrical spreading, key tool for computing the geometrical optics approximation.

Finally, we construct and implement a numerical scheme in the Eulerian framework for the eikonal equation. This Eulerian formulation applies also for the transport equation on the stretching matrix.

Keywords Hamilton-Jacobi equation; hyperbolic system; numerical scheme; asymptotic analysis; acoustic wave; high frequency regime.

AMS Subject Classification 35B40; 35L50; 65N06; 76Q05.

This work has been supported by EADS-Innovation Works through the funding of the PhD thesis of Y. Noumir.

Contents

1 Introduction

In this paper, we study the propagation of aeroacoustic perturbations, around a given mean flow, in the high frequency regime.

There are different ways of simulating the acoustic propagation using various formulations of the problem. One has, apart from the direct numerical simulation of the Partial Differential Equation (PDE), the integral equation method (where one solves through finite element methods a problem on the boundary [8]), the variational formulation (Discontinuous Galerkin method [35]), the Galbrun's equation (where, under suitable hypothesis on the mean flow, one obtains a scalar equation on the displacement field [28])... To have an accurate approximation of the solution in all these approaches, one must have, from a practical point of view, at least ten grid points per wavelength. Hence, in the high frequency regime, the number of unknowns is large, and the direct numerical simulation becomes very expensive. When the given mean flow and the sound velocity are slowly varying in space and time, an alternative is to use the *Linear Geometrical Optics* in the high frequency regime (see [22]), that we will outline now. It consists in replacing the solution by $a(x,k)e^{i(k\psi(x)-\omega t)}$, where $a(x,k) \sim \sum_{j\in\mathbb{N}} a_j(x)(ik)^{-j}$. Substituing this expansion into the wave equation, and setting to zero all the terms in powers of ik, we obtain a nonlinear equation for the phase ψ called the *Eikonal equation* which is an Hamilton-Jacobi equation. The coefficients a_j of the asymptotic expansion are determined iteratively by an evolution equation with source terms. There is a substantial literature in the resolution of the wave equation in the high frequency regime, and the article of Engquist and Runborg [10] provides a useful overview and a good source for references.

In the linear geometrical optics approximation, it is generally also assumed that the wavelength is small compared to the structure scale. However, one can find results that take into account geometric singularities: the diffraction problems for electromagnetic waves (Bouche and Molinet [4]) or the scattering theory for hyperbolic systems (Keller [23]).

The ratio between the wavelength and the characteristic length of the phenomena studied is also important. When it is of order 1, the Linear Geometrical Optics breaks down. The difficulty is due to the fact that the proposed approximations of the solutions satisfy the equations up to a remainder term that is not really small compared to the physical scale. In this case, one can use the *Nonlinear Geometrical Optics* ([16, 20, 21] among many references). Our paper does not address this limit.

Together with theoretical analysis, finding an efficient numerical scheme to solve the equations, obtained under the high frequency approximation, is also a very active field of research. There are mainly two approaches. The first classical trend consists in determining the trajectory of the rays and then solve the eikonal and the transport equations along these rays as ordinary differential equations. The second trend is to solve directly the eikonal and the transport equations as PDEs. This second approach to calculate solutions of Hamilton-Jacobi equations has been used in a wide range of applications: the optimal control (Crandall, Lions [7]), the shape-from-shading problem (Rouy, Tourin [37]), the electromagnetics wave propagation in the high frequency regime (Benamou *et al.* [2])... The study of the numerical methods, for solving the Hamilton-Jacobi equation as a PDE, is an active area of research.

This contribution is devoted to the study of high-frequency propagation of the acoustic wave in a moving flow. We use an Eulerian approach. The mathematical representation chosen to model this problem is the system of Entropic-Euler equations. The unknown of the problem is a perturbation of a mean flow, which leads naturally to consider the linearized equations. The mean velocity is assumed to be smooth and subsonic, it can be non-uniform or non-potential. The system on the perturbation is hyperbolic symmetrizable of order 1 in the sense of Friedrichs [11]. It is also equivalent, for smooth solutions, to the usual system of Euler equations for conservation of mass, momentum, and total energy (Landau and Lifchitz [25]). In the sequel, this system and equivalent systems will be called the Euler equations.

The construction of the asymptotic solutions for such a system was given first in the article of Lax [26], and a complete synthesis can be read in the book of Rauch [36]. We apply these general results to our system. We give the explicit equations that one has to solve for the computation of the geometrical optics approximation of the perturbation, namely the eikonal equation on the phase, and the transport equation on the leading term of the asymptotic expansion. We show here that the latter turns into a scalar conservative transport equation along the group velocity. This generalizes a known result of the high frequency acoustics in the absence of flow in the high frequency regime (see Theorem 2.11). We do not use this conservative transport equation for the numerical resolution but rather an equivalent approach using the geometrical spreading introduced in a natural fashion by Benamou *et al.* [3] for the wave equation, and which appears to be the key tool also in this more general situation. It is straightforward to deduce from this geometrical spreading the acoustic pressure and the acoustic velocity perturbations.

The article is organized as follows. **In section 1**, we derive a conservative scalar transport equation along the group velocity. Then we compute, for any type of regular mean flow, the leading order term of the asymptotic expanstion of the acoustic perturbation. **In section 2**, we introduce the geometrical spreading related to our system. A transport equation in the Eulerian formulation is derived. **In section 3**, we develop a numerical scheme of second order in space and time to approximate the solution of the eikonal equation on the phase. This scheme is tested and the convergence order verified. We perform a detailed comparaison between the analytical solution and the numerical solution in non trivial cases. **In section 4**, we develop a method for computing the geometrical spreading, through the introduction of a matrix, called the stretching matrix, which characterizes the spreading of rays. A comparaison with non trivial analytical solutions is also presented for the computation of the amplitude.

2 Conservative transport equation

Assume that the fluid is a inviscid perfect gas. Assume that we choose the Froude number such that the gravity is negligible, and that there is no thermal diffusion. The Entropic-Euler equations for mass, momentum, and entropy density are written:

$$\left\{\begin{array}{rcl} \partial_t \rho + \mathrm{div}_{\boldsymbol{x}}(\rho \boldsymbol{u}) &=& 0 \\ \partial_t(\rho \boldsymbol{u}) + \mathrm{div}_{\boldsymbol{x}}\left(\rho \boldsymbol{u}\otimes\boldsymbol{u} + p I_d\right) &=& 0 \\ \partial_t(\rho s) + \mathrm{div}_{\boldsymbol{x}}(\rho s \boldsymbol{u}) &=& 0 \end{array}\right. , \tag{1}$$

where ρ denotes the mass density, $\boldsymbol{u} = (u_1, \cdots, u_d)$ the velocity of the fluid, s the entropy, and $p = \rho^\gamma e^s$ the pressure, γ being the perfect gas constant. The space-time variable is denoted by $\boldsymbol{y} = (t, \boldsymbol{x}) \in \mathbb{R}_t \times \mathbb{R}^d$ with $t = y_0$ and $\boldsymbol{x} = (x_1, \cdots, x_d)$.

2.1 Linearization of Euler equations

The aeroacoustic model is based on perturbations of a reference solution $W_0 = (\rho_0, \rho_0 \boldsymbol{u}_0, \rho_0 s_0)^t$ of the system (1). Throughout this paper, we assume that the mean profile W_0 is a smooth function. The perturbed quantities, or acoustic

quantities, $W=(\varrho,\boldsymbol{q},\mathcal{s})^t$ are defined through

$$\left\{\begin{array}{ll}\rho & =\rho_0+\varrho\\ \rho\boldsymbol{u} & =\rho_0\boldsymbol{u}_0+\boldsymbol{q}\\ \rho s & =\rho_0 s_0+\mathcal{s}\end{array}\right. . \tag{2}$$

The linear system obtained by linearization of the Euler equations around the given reference solution W_0 is:

$$\left\{\begin{array}{l}\partial_t\varrho+\mathrm{div}_{\boldsymbol{x}}\boldsymbol{q}=0\\ \\ \partial_t\boldsymbol{q}+\mathrm{div}_{\boldsymbol{x}}\left(\boldsymbol{u}_0\otimes\boldsymbol{q}+\boldsymbol{q}\otimes\boldsymbol{u}_0-\varrho\,\boldsymbol{u}_0\otimes\boldsymbol{u}_0\right)+\boldsymbol{\nabla}_{\boldsymbol{x}}\left(\left(\mathrm{c}_0^2-\dfrac{\mathrm{p}_0\mathrm{s}_0}{\rho_0}\right)\varrho+\dfrac{\mathrm{p}_0}{\rho_0}\mathcal{s}\right)=0\\ \\ \partial_t\mathcal{s}+\mathrm{div}_{\boldsymbol{x}}\left(\mathcal{s}\,\boldsymbol{u}_0+s_0\boldsymbol{q}-s_0\varrho\,\boldsymbol{u}_0\right)=0\end{array}\right. , \tag{3}$$

where $c_0=\sqrt{\dfrac{\gamma p_0}{\rho_0}}$ is the sound velocity. We assume that the mean flow is **subsonic**, *i.e.* $|\boldsymbol{u}_0|<c_0$.

The equations above on the perturbed quantities can be rewritten

$$L(\boldsymbol{y},\partial_{\boldsymbol{y}})W=0, \tag{4}$$

where $L(\boldsymbol{y},\partial_{\boldsymbol{y}})$ is the linear differential matricial operator of order 1, with coefficients $(A_i)_{1\le i\le d}$ (real square $(d+2)\times(d+2)$ matrices *cf.* (10)) depending on the mean profile $W_0=(\rho_0,\rho_0\boldsymbol{u}_0,\rho_0 s_0)^t$, given by

$$L(\boldsymbol{y},\partial_{\boldsymbol{y}})=I_{d+2}\partial_t+\sum_{i=1}^{d}A_i(\boldsymbol{y})\partial_{x_i}+\sum_{i=1}^{d}\partial_{x_i}A_i(\boldsymbol{y}).$$

Remark 2.1. *Notice that the operator $L(\boldsymbol{y},\partial_{\boldsymbol{y}})$ is **symmetrizable hyperbolic** in the sense of Friedrichs [11], i.e. there exists a symmetric positive definite matrix A_0 and regular in its arguments such that the matrices $(A_0A_i)_{1\le i\le d}$ are symmetric.*

Throughout this paper, we denote by Γ_{inc} a smooth hypersurface in $\mathbb{R}^d$, and let Ω be the open subset of $\mathbb{R}^d$ which lies on one side of Γ_{inc}. Set $\mathcal{T}=\mathbb{R}_t\times\Omega$, and define $\Sigma_{inc}=\mathbb{R}_t\times\Gamma_{inc}$. We shall also use the notation $\mathbf{y}_0=(t,\mathbf{x}_0)$ for $\mathbf{x}_0\in\Gamma_{inc}$.

The tangent bundle of $\mathcal{T}$ is $T\mathcal{T}$. A fiber over $\boldsymbol{y}\in\mathcal{T}$ of this bundle is the tangent vector space $T_{\boldsymbol{y}}\mathcal{T}$ of $\mathcal{T}$ at $\boldsymbol{y}$. In the same way, the cotangent bundle $T^*\mathcal{T}$ (or phase space) consists of fibers over $\boldsymbol{y}$ each of which is the dual vector

space to $T_{\mathbf{y}}\mathscr{T}$. The cotangent bundle admits a canonical symplectic structure given by $w = \mathrm{d}\alpha$ where α is the Liouville form, we denote its coordinates by $(\boldsymbol{y},\boldsymbol{\eta}) \equiv (t,\boldsymbol{x},\tau,\boldsymbol{\xi})$.

We require the *inflow* condition on Γ_{inc}, *i.e.* $\boldsymbol{u}_0.\boldsymbol{\nu} > 0$ where $\boldsymbol{\nu}$ is the inward normal to Ω.

We consider the equations (4) in $\mathscr{T}$ together with the incident boundary condition on Σ_{inc}:

$$\begin{pmatrix} \rho \\ \boldsymbol{q} \end{pmatrix}(\mathbf{y}_0) = \begin{pmatrix} a^+_{inc} \\ \boldsymbol{b}^+_{inc} \end{pmatrix}(\mathbf{y}_0,k)e^{ik\varphi^+_{inc}(\mathbf{y}_0)} + \begin{pmatrix} a^-_{inc} \\ \boldsymbol{b}^-_{inc} \end{pmatrix}(\mathbf{y}_0,k)e^{ik\varphi^-_{inc}(\mathbf{y}_0)}, \tag{5}$$

where $\varphi^{\pm}_{inc}$, $a^{\pm}_{inc}$, and $\boldsymbol{b}^{\pm}_{inc}$ are functions in $\mathscr{C}^{\infty}(\Sigma_{inc})$. Moreover, $a^{\pm}_{inc}$, and $\boldsymbol{b}^{\pm}_{inc}$ have an asymptotic expansion of the form (7), and $k >> 1$ is the wave number. The incident phase φ_{inc} satisfies the compatibility conditions (**H**.a) given below, and the leading term of the asymptotic expansion of $\boldsymbol{b}^{\pm}_{inc}(.,k)$ satisfies the polarisation condition (16) given later. Furthermore, the terms of the asymptotic expansion of $\boldsymbol{b}^{\pm}_{inc}(.,k)$ and $a^{\pm}_{inc}(.,k)$ must verify some compatibility conditions that we will not specify here (see [36]).

Note that the surface Γ_{inc} is not characteristic. Indeed the characteristic polynomial of the matrix $A_\nu = \sum_{j=1}^{d} \nu_j A_j$, where ν_j are the components of $\boldsymbol{\nu}$, is (see proof of Proposition 2.4):

$$\det(A_\nu - \lambda I_{d+2}) = (\boldsymbol{u}_0.\boldsymbol{\nu} - \lambda)^d \left((\boldsymbol{u}_0.\boldsymbol{\nu} - \lambda)^2 - c_0^2 \right).$$

Under the hypothesis mentionned above, the matrix A_ν is invertible and its eigenvalues are:

- $\lambda_0 = \boldsymbol{u}_0.\boldsymbol{\nu} > 0$ with multiplicity d.
- the simple eigenvalues: $\lambda_+ = \boldsymbol{u}_0.\boldsymbol{\nu} + c_0 > 0$ and $\lambda_- = \boldsymbol{u}_0.\boldsymbol{\nu} - c_0 < 0$.

Also, note that from [12], the hyperbolic boundary value problem (4)-(5) is well posed.

2.2 High frequency approximation

In the high frequency regime, the oscillatory behavior of the solution makes too expensive to perform the direct numerical simulation. However, when the wave number k is much larger than the magnitude of the variations of the mean quantities, the notion of asymptotic solution provides an alternative for the

prediction of the oscillatory behavior of the solution. In this subsection, we present the equations governing the propagation of oscillating solutions of the operator $L(\boldsymbol{y},\partial_y)$. The rigorous study for the construction of asymptotic solutions for hyperbolic systems was begun by the paper of Lax [26], also the works of Keller [22] and Friedlander [14], and subsequently the work of Ludwig [30] for the case of the caustics among many other authors. Under regularity assumptions on the mean flow W_0, there is existence and uniqueness of the asymptotic solution of type (6) below for the operator $L(\boldsymbol{y},\partial_y)$ with oscillating Cauchy data.

Definition 2.2. *We say that $W(\boldsymbol{y},k)$ is an **asymptotic solution** of the operator $L(\boldsymbol{y},\partial_y)$ if:*

$$L(\boldsymbol{y},\partial_y)W(\boldsymbol{y},k)=O(k^{-\infty}),$$

where $k>>1$ and $O(k^{-\infty})$ denotes a function which is more quickly decreasing than any power of k uniformly on any compact set of $\mathbb{R}_t\times\mathbb{R}^d$.

Here, we seek an asymptotic solution of the operator $L(\boldsymbol{y},\partial_y)$ as a classical **Ansatz**, *i.e.*

$$W(\boldsymbol{y},k)=\begin{pmatrix}\varrho\\ \boldsymbol{q}\\ \mathfrak{s}\end{pmatrix}(\boldsymbol{y},k)\simeq \mathscr{W}(\boldsymbol{y},k)e^{ik\phi(y)}, \tag{6}$$

where the amplitude $\mathscr{W}(.,k)$ has an asymptotic expansion in inverse powers of ik:

$$\mathscr{W}(\boldsymbol{y},k)=\sum_{j=0}^{\infty}\frac{1}{(ik)^j}\mathscr{W}_j(\boldsymbol{y})=\sum_{j=0}^{\infty}\frac{1}{(ik)^j}\begin{pmatrix}a_j(\boldsymbol{y})\\ \boldsymbol{b}_j(\boldsymbol{y})\\ d_j(\boldsymbol{y})\end{pmatrix}. \tag{7}$$

The phase ϕ, as well as $\mathscr{W}_j$, are assumed to be smooth real valued functions. We also assume that $\boldsymbol{\nabla}_y\phi\neq\boldsymbol{0}$ in the whole computational domain. The relation $\simeq$, in the expression (6), is understood in the sense that for all $J\in\mathbb{N}$, for any multi-index $\alpha\in\mathbb{N}^i$, and for any compact set K of $\mathscr{T}$, there exists a constant $C(K,J,\alpha)$ such that:

$$\left|\partial^{\alpha}_{\boldsymbol{y}^{\alpha}}\left(W(\boldsymbol{y},k)-\sum_{j=0}^{J-1}\frac{1}{(ik)^j}\mathscr{W}_j(\boldsymbol{y})e^{ik\phi(y)}\right)\right|\leq C(K,J,\alpha)k^{-J},\quad\forall\boldsymbol{y}\in K. \tag{8}$$

There is no requirement that the asymptotic series is convergent when j tends to infinity, but it must approaches the W and all its derivatives with a remainder term of the order of the truncation in the sense of (8). Note that this asymptotic expansion is not unique (*e.g.* [19]).

Definition 2.3. ***The geometrical optics approximation*** *consists in considering only the leading order term as a good approximation of the solution, i.e.*

$$W(\boldsymbol{y},k)\simeq\left(\mathscr{W}_0(\boldsymbol{y})+O(k^{-1})\right)e^{ik\phi(\boldsymbol{y})}.$$

Formally, replacing the acoustic perturbation by its asymptotic approximation (6) in (4) and ordering in powers of ik, we find that the terms of the asymptotic expansion satisfy the system of equations:

$$\begin{cases} L_1(\boldsymbol{y},\boldsymbol{\nabla}_y\phi)\mathscr{W}_0=0 & \text{(9a)}\\ \\ L_1(\boldsymbol{y},\boldsymbol{\nabla}_y\phi)\mathscr{W}_{j+1}+L(\boldsymbol{y},\partial_y)\mathscr{W}_j=0,\quad j\geq 0. & \text{(9b)}\end{cases}$$

where $L_1(\boldsymbol{y},\boldsymbol{\eta})=\tau I_{d+2}+\sum_{\mu=1}^{d}\xi_\mu A_\mu(\boldsymbol{x})$ is **the principal symbol** of the operator $L(\boldsymbol{y},\partial_y)$.

Introduce the set $\Lambda_0=\{(\boldsymbol{y},\boldsymbol{\eta})\in T^*\mathscr{T}\setminus\{0\}\,;\,\det(L_1(\boldsymbol{y},\boldsymbol{\eta}))=0\}$ and the set $\Lambda_\phi=\left\{(\boldsymbol{y},\boldsymbol{\nabla}_y\phi)\,;\,\boldsymbol{y}\in\mathscr{T}\right\}$. The sets Λ_0 and Λ_ϕ are respectively called the **characteristic variety** associated to the operator $L(\boldsymbol{y},\partial_y)$ and the **Lagrangian manifold** generated by the phase ϕ.

It can be checked that

$$L_1(\boldsymbol{y},\boldsymbol{\eta})=\begin{pmatrix}\tau & {}^t\xi & 0\\ \left(c_0^2-\dfrac{p_0s_0}{\rho_0}\right)\xi-\left(\boldsymbol{u}_0.\xi\right)\boldsymbol{u}_0 & (\tau+\boldsymbol{u}_0.\xi)I_d+\boldsymbol{u}_0\otimes\xi & \dfrac{p_0}{\rho_0}\xi\\ -s_0\,\boldsymbol{u}_0.\xi & s_0\,{}^t\xi & \tau+\boldsymbol{u}_0.\xi\end{pmatrix}, \tag{10}$$

where $\otimes$ denotes the tensor product (recall that the tensor product of two vectors $\boldsymbol{u}$ and $\boldsymbol{v}$ is the matrix whose entries are $(\boldsymbol{u}\otimes\boldsymbol{v})_{i,j}=u_iv_j$). Note that one can obtain the matrices $(A_i)_{1\leq i\leq d}$ from this expression.

For $\epsilon\in\{-1,0,1\}$, we introduce the Hamiltonian $\mathscr{H}^\epsilon$ defined by:

$$\mathscr{H}^\epsilon(\boldsymbol{y},\boldsymbol{\eta})=\tau+\xi.\boldsymbol{u}_0(\boldsymbol{y})+\epsilon c_0(\boldsymbol{y})|\xi|. \tag{11}$$

For $(\boldsymbol{y},\xi)\in\mathscr{T}\times T^*_{\boldsymbol{x}}\Omega$, we denote by $\tau(\boldsymbol{y},\xi)$ an eigenvalue of the matrix $\sum_{i=1}^{d}\xi_iA_i(\boldsymbol{y})$, *i.e.* there exists $\epsilon\in\{-1,0,1\}$ such that $\mathscr{H}^\epsilon(\boldsymbol{y},\tau(\boldsymbol{y},\xi),\xi)=0$. **The group velocity** is then defined by $\boldsymbol{v}_g=-\boldsymbol{\nabla}_\xi\tau(\boldsymbol{y},\xi)$.

Proposition 2.4. *There exists a non trivial solution of (9a) if and only if there exists $\epsilon \in \{-1,0,1\}$ such that the phase ϕ is solution of the Hamilton-Jacobi equation $\mathscr{H}^\epsilon(\boldsymbol{y},\boldsymbol{\nabla}_y\phi(\boldsymbol{y}))=0$. The leading order term of (7) is thus an eigenvector of the matrix $\sum_{i=1}^d \xi_i A_i(\boldsymbol{y})$ associated with the eigenvalue $-\partial_t\phi(\boldsymbol{y})$.*

Proof. This is simply due to the fact that the linear system has a non trivial solution $\mathscr{W}_0$ if and only if: $\det(L_1(\boldsymbol{y},\boldsymbol{\nabla}_y\phi))=\left(\mathscr{H}^{0\,d}\,\mathscr{H}^{+}\mathscr{H}^{-}\right)(\boldsymbol{y},\boldsymbol{\nabla}_y\phi)=0$, and that the leading term is in the kernel of the matrix $L_1(\boldsymbol{y},\boldsymbol{\nabla}_y\phi)$. □

The equation on the phase ϕ is called the **Eikonal equation**. We have:

- On the one hand, the equation $(\partial_t\phi+\boldsymbol{u}_0.\boldsymbol{\nabla}_x\phi)^2=c_0^2|\boldsymbol{\nabla}_x\phi|^2$, which characterizes the **acoustic modes** $(\mathscr{H}^\epsilon(\boldsymbol{y},\boldsymbol{\nabla}_y\phi))=0\,;\,\epsilon=\pm1)$.
- On the other hand, the equation $\partial_t\phi+\boldsymbol{u}_0.\boldsymbol{\nabla}_x\phi=0$, which corresponds to **the vortical and entropic modes** $(\mathscr{H}^\epsilon(\boldsymbol{y},\boldsymbol{\nabla}_y\phi))=0\,;\,\epsilon=0)$.

Remark 2.5. *In what follows, we focus specifically on the acoustic modes. We deal especially with their geometrical optics approximation. The entropic and vortical modes are only convected by the mean flow, and we are not interested by them in this study.*

The following results of this section are written in the Hamiltonian formalism. The classical results, recalled in what follows, are exposed with detailed proofs in [41] or [18].

Definition 2.6. *The **bicharacteristics** are the integral curves in $T^*\mathscr{T}$ for the Hamiltonian field $(\mathscr{H}_{\boldsymbol{\eta}},-\mathscr{H}_{\boldsymbol{y}})$ that is:*

$$\left\{\begin{array}{rcl}\dot{\boldsymbol{y}}(s,\boldsymbol{\beta}) &=& \mathscr{H}_{\boldsymbol{\eta}}(\boldsymbol{y}(s,\boldsymbol{\beta}),\boldsymbol{\eta}(s,\boldsymbol{\beta}))\\ \dot{\boldsymbol{\eta}}(s,\boldsymbol{\beta}) &=& -\mathscr{H}_{\boldsymbol{y}}(\boldsymbol{y}(s,\boldsymbol{\beta}),\boldsymbol{\eta}(s,\boldsymbol{\beta}))\end{array}\right. \quad \textit{with} \quad \left\{\begin{array}{l}\boldsymbol{y}(0,\boldsymbol{\beta})=\mathbf{y}_0(\boldsymbol{\beta})\\ \boldsymbol{\eta}(0,\boldsymbol{\beta})=\boldsymbol{\eta}_0(\boldsymbol{\beta})\end{array}\right., \tag{12}$$

where $\dot{}$ denotes the derivative with respect to the parameter s along the bicharacteristics, $\mathscr{H}_{\boldsymbol{\eta}}$ (resp. $\mathscr{H}_{\boldsymbol{y}}$) is the derivative of the Hamiltonian $\mathscr{H}$ with respect to $\boldsymbol{\eta}$ (resp. to $\boldsymbol{y}$), $\boldsymbol{\beta}=(t_0,\boldsymbol{\alpha})\in\mathbb{R}_t\times\mathbb{R}^{d-1}$ characterizes a point $\mathbf{y}_0(\boldsymbol{\beta})=(t_0,\mathbf{x}_0(\boldsymbol{\alpha}))$ on the incident surface Σ_{inc} (where $\mathbf{x}_0$ is a parameterization of Γ_{inc}), and $\boldsymbol{\eta}_0(\boldsymbol{\beta})\in T^*_{\mathbf{y}_0(\boldsymbol{\beta})}\mathscr{T}$.

The **rays** are defined as the projection of the bicharacteristics on the configuration space, *i.e.* $\big(\boldsymbol{y}(s,\boldsymbol{\beta}),\boldsymbol{\eta}(s,\boldsymbol{\beta})\big)\longrightarrow\boldsymbol{y}(s,\boldsymbol{\beta})$.

The Hamiltonian system (12) is coupled with **the Lagrangian phase** φ which verifies the equation

$$\dot{\varphi}(s,\boldsymbol{\beta})=\boldsymbol{\eta}(s,\boldsymbol{\beta}).\mathscr{H}_{\boldsymbol{\eta}}(\boldsymbol{y}(s,\boldsymbol{\beta}),\boldsymbol{\eta}(s,\boldsymbol{\beta}))-\mathscr{H}(\boldsymbol{y}(s,\boldsymbol{\beta}),\boldsymbol{\eta}(s,\boldsymbol{\beta})). \tag{13}$$

Remark 2.7. *The Lagrangian phase φ is constant along the bicharacteristics for an homogeneous Hamiltonian $\mathscr{H}$ of degree 1 (i.e. $\mathscr{H} = \boldsymbol{\eta}.\mathscr{H}_{\boldsymbol{\eta}}$). This is the case of the Hamiltonian $\mathscr{H}^{\epsilon}$. This property shall be the key tool of the calculus of an explicit phase which will be our reference solution to test the numerical schemes developed later.*

Given the incident phase φ_{inc} on Σ_{inc}, we consider the boundary value problem $\varphi(0,\boldsymbol{\beta}) = \varphi_{inc}(t_0, \mathbf{x}_0(\boldsymbol{\alpha}))$. We say that the initial condition $\boldsymbol{\eta}_0$ is **compatible** with the Lagrangian incident phase φ_{inc} if:

((**H**.a).1) $\tau_0(\boldsymbol{\beta}) = \partial_t \varphi_{inc}(t_0, \mathbf{x}_0(\boldsymbol{\alpha}))$,

((**H**.a).2) for all $\mathbf{x}_0(\boldsymbol{\alpha}) \in \Gamma_{inc}$ and $\boldsymbol{\nu} \in T_{\mathbf{x}_0(\boldsymbol{\alpha})}\Gamma_{inc}$, we have

$$\mathrm{d}_{\mathbf{x}_0(\boldsymbol{\alpha})}\widetilde{\varphi}^{t_0}(\boldsymbol{\nu}) = \boldsymbol{\xi}_0(\boldsymbol{\beta}).\boldsymbol{\nu} \ \text{ with } \ \widetilde{\varphi}^{t_0}(\mathbf{x}_0(\boldsymbol{\alpha})) = \varphi_{inc}(t_0, \mathbf{x}_0(\boldsymbol{\alpha})),$$

((**H**.a).3) $\big(\mathbf{y}_0(\boldsymbol{\beta}), \boldsymbol{\eta}_0(\boldsymbol{\beta})\big)$ belongs to the characteristic variety Λ_0.

We assume **the transversality condition**, *i.e.* $\mathscr{H}_{\xi}\big(\mathbf{y}_0(\boldsymbol{\beta}), \boldsymbol{\eta}_0(\boldsymbol{\beta})\big)$ is not tangent to Γ_{inc} at $\mathbf{x}_0(\boldsymbol{\alpha})$. Furthermore, we assume that the initial bicharacteristic is *ingoing* into the domain $\mathscr{T}$, *i.e.*

(**H**.b) $\mathscr{H}_{\xi}(\mathbf{y}_0(\boldsymbol{\beta}), \boldsymbol{\eta}_0(\boldsymbol{\beta})).\boldsymbol{\nu}(\mathbf{x}_0(\boldsymbol{\alpha})) > 0$, where $\boldsymbol{\nu}$ is the inward normal to Ω.

Remark 2.8. *If the incident boundary is given by the equation $\Psi(\boldsymbol{x}) = 0$ where Ψ is a smooth function, the condition (**H**.b) is written $\{\Psi, \mathscr{H}\}_{|\Psi=\mathscr{H}=0} > 0$ where $\{\Psi, \mathscr{H}\} = \sum_{i=1}^{d} \left(\partial_{x_i}\Psi \mathscr{H} \partial_{x_i} - \partial_{\xi_i}\Psi \partial_{x_i}\mathscr{H}\right)$ is the Poisson bracket.*

Under the transversality condition, there exist a neighborhood $\mathscr{U}$ of $(s,\boldsymbol{\beta}) \in \mathbb{R} \times \left(\mathbb{R}_t \times \mathbb{R}^{d-1}\right)$ and a neighborhood $\mathscr{V} \subset \mathscr{T}$ of $\mathbf{y}_0(\boldsymbol{\beta}) \in \Sigma_{inc}$ such that the transformation from Lagrangian to Eulerian coordinates, *i.e.* $\mathscr{U} \ni (s,\boldsymbol{\beta}) \to \boldsymbol{y}(s,\boldsymbol{\beta}) \in \mathscr{V}$, is a diffeomorphism (*e.g.* [18]). Thus the Lagrangian phase φ defines locally an **Eulerian phase** ϕ through $\phi(\boldsymbol{y}(s,\boldsymbol{\beta})) = \varphi(s,\boldsymbol{\beta})$, and ϕ is solution of the Hamilton-Jacobi equation $\mathscr{H}\left(\boldsymbol{y}, \boldsymbol{\nabla}_{\boldsymbol{y}}\phi(\boldsymbol{y})\right) = 0$.

Recall the classical result below which allows to identify the gradient of the solution of the eikonal equation with an element of $T^*\mathbb{R}^{d+1}$.

Proposition 2.9. *If ϕ solves the Hamilton-Jacobi equation $\mathscr{H}\left(\boldsymbol{y}, \boldsymbol{\nabla}_{\boldsymbol{y}}\phi(\boldsymbol{y})\right) = 0$, and if a bicharacteristic intersects the Lagrangian submanifold Λ_{ϕ} associated to ϕ, then it is contained in Λ_{ϕ}.*

Proof. Let $\big(\boldsymbol{y}(s,\boldsymbol{\beta}),\boldsymbol{\eta}(s,\boldsymbol{\beta})\big)\in\Lambda_0$ be a bicharacteristic that intersects Λ_ϕ. Hence there exist $(s_1,\boldsymbol{\beta}_1)$ and $(s_2,\boldsymbol{\beta}_2)$ in $\mathbb{R}\times(\mathbb{R}_t\times\mathbb{R}^{d-1})$ such that

$$\big(\boldsymbol{y}(s_1,\boldsymbol{\beta}_1),\boldsymbol{\eta}(s_1,\boldsymbol{\beta}_1)\big)\equiv\Big(\boldsymbol{y}(s_2,\boldsymbol{\beta}_2)),\boldsymbol{\nabla}_y\phi(\boldsymbol{y}(s_2,\boldsymbol{\beta}_2))\Big)\,. \tag{14}$$

Let $\tilde{\boldsymbol{y}}$ be the solution of the differential equation

$$\dot{\tilde{\boldsymbol{y}}}(s,\boldsymbol{\beta}_1)=\mathscr{H}_\eta\left(\tilde{\boldsymbol{y}}(s,\boldsymbol{\beta}_1),\boldsymbol{\nabla}_y\phi(\tilde{\boldsymbol{y}}(s,\boldsymbol{\beta}_1))\right),$$

with the condition $\tilde{\boldsymbol{y}}(s_1,\boldsymbol{\beta}_1)=\boldsymbol{y}(s_2,\boldsymbol{\beta}_2)$. Denote by $\tilde{\boldsymbol{\eta}}(s,\boldsymbol{\beta}_1)=\boldsymbol{\nabla}_y\phi(\tilde{\boldsymbol{y}}(s,\boldsymbol{\beta}_1))$. Differentiate the equation $\mathscr{H}\left(\tilde{\boldsymbol{y}}(s,\boldsymbol{\beta}_1),\boldsymbol{\nabla}_y\phi(\tilde{\boldsymbol{y}}(s,\boldsymbol{\beta}_1))\right)=0$ with respect to s, we get $\dot{\tilde{\boldsymbol{\eta}}}(s,\boldsymbol{\beta}_1)=-\mathscr{H}_y\left(\tilde{\boldsymbol{y}}(s,\boldsymbol{\beta}_1),\tilde{\boldsymbol{\eta}}(s,\boldsymbol{\beta}_1)\right)$. We deduce then that $(\boldsymbol{y},\boldsymbol{\eta})$ and $(\tilde{\boldsymbol{y}},\tilde{\boldsymbol{\eta}})$ are solutions of the same Hamiltonian system with the common point (14). We conclude using the uniqueness of the solution of the ODE system. □

Remark 2.10. *Note that for the acoustic modes,* ***the material derivative****, i.e.* $\mathrm{D}_t\phi^\pm=\partial_t\phi^\pm+\boldsymbol{u}_0.\boldsymbol{\nabla}_x\phi^\pm$*, of the phase* $\phi^\pm$ *along the mean flow* $\boldsymbol{u}_0$ *is not zero, that is* $\boldsymbol{\nabla}_x\phi^\pm\neq0$*. Indeed, if we suppose that* $D_t\phi^\pm=0$*, it follows that* $\boldsymbol{\nabla}_x\phi^\pm=0$ *by the eikonal equation* $\mathscr{H}^\pm=0$*, then* $\partial_t\phi^\pm=0$*, and hence* $\boldsymbol{\nabla}_y\phi^\pm=0$ *which is in contradiction with the hypothesis* $\boldsymbol{\nabla}_y\phi^\pm\neq0$*.*

2.3 Conservative transport equation for the acoustic pressure

In what follows up to the end of this paper, we deal only with the geometrical optics approximation of the acoustic modes in the Euler equations, although some results have a more general scope and are not limited to this case. Recall that $\phi^\pm$ is the solutions of the eikonal equations associated to the acoustic modes, *i.e.* $\mathscr{H}^\pm(\boldsymbol{y},\boldsymbol{\nabla}_y\phi^\pm)=0$.

Recall also that, from (9a), the leading order term $\mathscr{W}_0^\pm$ belongs to the kernel matrix $L_1(\boldsymbol{y},\boldsymbol{\nabla}_y\phi^\pm)$. Hence, it is easy, thanks to $\mathrm{D}_t\phi^\pm\neq0$ (see Remark 2.10), to check that $\mathscr{W}_0^\pm=a_0^\pm\left(1,\boldsymbol{v}_g^\pm,s_0\right)^t$, where the group velocity is written $\boldsymbol{v}_g^\pm=\boldsymbol{u}_0+c_0\boldsymbol{w}_g^\pm$ and $\boldsymbol{w}_g^\pm$ denotes the unit vector $\pm\dfrac{\boldsymbol{\nabla}_x\phi^\pm}{|\boldsymbol{\nabla}_x\phi^\pm|}$. Note that the **phase velocity** is $c_0\boldsymbol{w}_g^\pm$. The calculation of the term of the approximation of geometrical optics, for the acoustic modes, then reduces to the determination of $a_0^\pm$.

To establish the equation satisfied by the scalar function $a_0^\pm$, we introduce the projector $\Pi^\pm(\boldsymbol{y},\boldsymbol{\nabla}_y\phi^\pm)$ onto $\mathrm{Ker}(L_1(\boldsymbol{y},\boldsymbol{\nabla}_y\phi^{\ \pm}))$ along $\mathrm{Im}(L_1(\boldsymbol{y},\boldsymbol{\nabla}_y\phi^\pm))$. According to the system of equations (9b), we have

$$L(\boldsymbol{y},\partial_y)\mathscr{W}_0^\pm+L_1(\boldsymbol{y},\boldsymbol{\nabla}_y\phi^\pm)\mathscr{W}_1^\pm=0,$$

applying the projector $\Pi^{\pm}$ to the equation above yields

$$\Pi^{\pm} L(\boldsymbol{y}, \partial_y) \mathscr{W}_0^{\pm} = 0. \tag{15}$$

In the following Theorem, we prove that the equation (15) leads to a conservative equation on $a_0^{\pm}$. This corresponds to a well-known result for the scalar wave equation and Maxwell's equations, that we generalize here to a system of coupled equations. But before that, we give the polarization condition of the incident condition. For $\mathbf{y}_0 \in \Sigma_{inc}$, the polarization condition of the leading term of the asymptotic expansion of $\boldsymbol{b}_{inc}^{\pm}(., k)$ (given in (5)) is written:

$$\boldsymbol{b}_{inc}^{\pm}(\mathbf{y}_0, k) = \bar{a}_{inc}^{\pm}(\mathbf{y}_0) \boldsymbol{\nu}_{inc}^{\pm}(\mathbf{y}_0) + O(k^{-1}), \tag{16}$$

with $\boldsymbol{\nu}_{inc}^{\pm}(\mathbf{y}_0) = \boldsymbol{u}_0(\mathbf{y}_0) \pm c_0(\mathbf{y}_0) \dfrac{\boldsymbol{\xi}_0^{\pm}(\mathbf{y}_0)}{|\boldsymbol{\xi}_0^{\pm}(\mathbf{y}_0)|}$ where $\boldsymbol{\xi}_0^{\pm}$ verifies the compatibility conditions (**H**.a) with the incident phase φ_{inc}, and $\bar{a}_{inc}^{\pm}$ is the leading term of the asymptotic expansion of $a_{inc}^{\pm}(., k)$.

Theorem 2.11. *Assume that the compatibility (**H**.a) and transversality (**H**.b) conditions are verified, and that the hypothesis $\boldsymbol{\nabla}_y \phi^{\pm} \neq 0$ is satisfied. Assume, moreover, that the incident condition satisfies the polarization condition (16). Hence, there exists one and only one scalar function $a_0^{\pm}$, locally in vicinity of Σ_{inc}, solution of the conservative equation*

$$\partial_t \left(\frac{c_0 a_0^{\pm 2}}{\rho_0 |\boldsymbol{\nabla}_x \phi^{\pm}|} \right) + \operatorname{div} \left(\frac{c_0 a_0^{\pm 2}}{\rho_0 |\boldsymbol{\nabla}_x \phi^{\pm}|} \boldsymbol{\nu}_g^{\pm} \right) = 0, \tag{17}$$

with the incident condition $a_{0\,|\Sigma_{inc}}^{\pm} = \bar{a}_{inc}^{\pm}$, such that the leading terms of the acoustic modes are written as $\mathscr{W}_0^{\pm} = a_0^{\pm} \left(1\,,\, \boldsymbol{\nu}_g^{\pm}\,,\, s_0\right)^t$, and there exists $C > 0$ such that

$$\left| W(\boldsymbol{y}, k) - \mathscr{W}_0^{\pm}(\boldsymbol{y}) e^{ik\phi^{\pm}(\boldsymbol{y})} \right| \leq C k^{-1} \quad \textit{for} \quad \boldsymbol{y} \in \mathscr{T}.$$

Note that this formulation imposes compatibility conditions on all terms of the asymptotic expansion of $\boldsymbol{b}_{inc}^{\pm}(., k)$ (see (8)).

To prove Theorem 2.11, we need the following Lemma on the eikonal equation whose proof is given in appendix A:

Lemma 2.12. *If $\phi^{\pm}$ is a smooth solution of the eikonal equation $\mathscr{H}^{\pm}=0$ (equation (11) with $\epsilon=\pm 1$), then*

$$\partial_t\left(\frac{1}{|\boldsymbol{\nabla}_x\phi^{\pm}|}\right)+\boldsymbol{v}_g^{\pm}.\boldsymbol{\nabla}_x\left(\frac{1}{|\boldsymbol{\nabla}_x\phi^{\pm}|}\right)= \frac{1}{|\boldsymbol{\nabla}_x\phi^{\pm}|^3}\boldsymbol{\nabla}_x\phi^{\pm}.\left(\boldsymbol{\nabla}_x\phi^{\pm}\overline{\otimes}\overline{\nabla}_x\boldsymbol{u}_0\right)\pm\frac{1}{|\boldsymbol{\nabla}_x\phi^{\pm}|^2}\boldsymbol{\nabla}_x\phi^{\pm}.\boldsymbol{\nabla}_x c_0.$$

Proof of Theorem 2.11. Recall that the leading term $\mathscr{W}_0^{\pm}$ of the asymptotic expansion of the acoustic modes is $\mathscr{W}_0^{\pm}=a_0^{\pm}e_{\Pi^{\pm}}$, where $e_{\Pi^{\pm}}\equiv\left(1,\boldsymbol{v}_g^{\pm},s_0\right)^t$ is in the kernel of the matrix $L_1(\boldsymbol{y},\boldsymbol{\nabla}_{\boldsymbol{y}}\phi^{\pm})$ such that $\Pi^{\pm}\boldsymbol{e}_{\Pi^{\pm}}=\boldsymbol{e}_{\Pi^{\pm}}$.

Let $\boldsymbol{e}_{{}^t\Pi^{\pm}}$ be the unique element of $\mathrm{Ker}({}^tL_1(\boldsymbol{y},\boldsymbol{\nabla}_{\boldsymbol{y}}\phi^{\pm}))$ such that

$$\Pi^{\pm}=<\boldsymbol{e}_{{}^t\Pi^{\pm}},.>\boldsymbol{e}_{\Pi^{\pm}}\quad\text{and}\quad<\boldsymbol{e}_{{}^t\Pi^{\pm}},\boldsymbol{e}_{\Pi^{\pm}}>=1. \tag{18}$$

One can check that

$$\boldsymbol{e}_{{}^t\Pi^{\pm}}=\frac{1}{2c_0}\left(c_0-\boldsymbol{u}_0.\boldsymbol{w}_g^{\pm}-\frac{s_0c_0}{\gamma},\boldsymbol{w}_g^{\pm},\frac{c_0}{\gamma}\right)^t\in\mathbb{R}^{d+2}.$$

Using (18), the equation (15) turns into the following equation on $a_0^{\pm}$

$$\partial_t a_0^{\pm}+\sum_{i=1}^{d}<\boldsymbol{e}_{{}^t\Pi^{\pm}},A_i\boldsymbol{e}_{\Pi^{\pm}}>\partial_i a_0^{\pm}+<\boldsymbol{e}_{{}^t\Pi^{\pm}},L(\boldsymbol{y},\partial_y)\boldsymbol{e}_{\Pi^{\pm}}>a_0^{\pm}=0.$$

We note that (see [36]) we have $<\boldsymbol{e}_{{}^t\Pi^{\pm}},A_i\boldsymbol{e}_{\Pi^{\pm}}>=v_i^{\pm}$ where $v_i^{\pm}$ is the ith component of the group velocity $\boldsymbol{v}_g^{\pm}$. Indeed, the derivative of the equation $L_1\left(\boldsymbol{y},\tau(\boldsymbol{y},\boldsymbol{\xi}),\boldsymbol{\xi}\right)\boldsymbol{e}_{\Pi^{\pm}}\left(\boldsymbol{y},\tau(\boldsymbol{y},\boldsymbol{\xi}),\boldsymbol{\xi}\right)=0$ with respect to ξ_i gives

$$\partial_{\xi_i}\tau\,\boldsymbol{e}_{\Pi^{\pm}}+A_i\boldsymbol{e}_{\Pi^{\pm}}=\partial_{\xi_i}L_1(\boldsymbol{y},\boldsymbol{\eta})\boldsymbol{e}_{\Pi^{\pm}}=-L_1(\boldsymbol{y},\boldsymbol{\eta})\partial_{\xi_i}\boldsymbol{e}_{\Pi^{\pm}},$$

taking the scalar product of the equation above with $\boldsymbol{e}_{{}^t\Pi^{\pm}}$ yields the result owing to $v_i=-\partial_{\xi_i}\tau$.

It follows that

$$\partial_t a_0^{\pm}+\boldsymbol{v}_g^{\pm}.\boldsymbol{\nabla}_{\boldsymbol{x}}a_0^{\pm}+<\boldsymbol{e}_{{}^t\Pi^{\pm}},L(\boldsymbol{y},\partial_y)\boldsymbol{e}_{\Pi^{\pm}}>a_0^{\pm}=0. \tag{19}$$

On the one hand, we have $\partial_t\boldsymbol{e}_{\Pi^{\pm}}=\left(0,\partial_t\boldsymbol{u}_0+\partial_t(c_0\boldsymbol{w}_g^{\pm}),\partial_t s_0\right)^t$. On the other hand, we have $|\boldsymbol{w}_g^{\pm}|=1$, which implies

$$<\boldsymbol{e}_{{}^t\Pi^{\pm}},\partial_t\boldsymbol{e}_{\Pi^{\pm}}>=\frac{\boldsymbol{w}_g^{\pm}.\partial_t\boldsymbol{u}_0}{2c_0}+\frac{\partial_t c_0}{2c_0}+\frac{\partial_t s_0}{2\gamma}. \tag{20}$$

In the appendix B, we prove that

$$\sum_{i=1}^{d} < \boldsymbol{e}_{{}^t\Pi^\pm}, \partial_i(A_i \boldsymbol{e}_{\Pi^\pm}) >= \frac{\mathrm{div}\boldsymbol{v}_g^\pm}{2} - \frac{\boldsymbol{v}_g^\pm.\boldsymbol{\nabla}_{\boldsymbol{x}}\rho_0}{2\rho_0} + \frac{\boldsymbol{v}_g^\pm.\boldsymbol{\nabla}_{\boldsymbol{x}}c_0}{2c_0}$$
$$+ \frac{\boldsymbol{w}_g^\pm.\left(\boldsymbol{w}_g^\pm \bar{\otimes} \bar{\bar{\nabla}}_x \boldsymbol{u}_0 + \boldsymbol{\nabla}_{\boldsymbol{x}} c_0\right)}{2} - \frac{\partial_t \rho_0}{2\rho_0} - \frac{\boldsymbol{w}_g^\pm.\partial_t \boldsymbol{u}_0}{2c_0} - \frac{\partial_t s_0}{2\gamma}. \quad (21)$$

Combining (20) and (21), we obtain

$$< \boldsymbol{e}_{{}^t\Pi^\pm}, L(\boldsymbol{y}, \partial_{\boldsymbol{y}})\boldsymbol{e}_{\Pi^\pm} >= \frac{\mathrm{div}\boldsymbol{v}_g^\pm}{2} - \frac{\boldsymbol{v}_g^\pm.\boldsymbol{\nabla}_{\boldsymbol{x}}\rho_0}{2\rho_0} + \frac{\boldsymbol{v}_g^\pm.\boldsymbol{\nabla}_{\boldsymbol{x}}c_0}{2c_0}$$
$$+ \frac{\boldsymbol{w}_g^\pm.\left(\boldsymbol{w}_g^\pm \bar{\otimes} \bar{\bar{\nabla}}_x \boldsymbol{u}_0 + \boldsymbol{\nabla}_{\boldsymbol{x}} c_0\right)}{2} - \frac{\partial_t \rho_0}{2\rho_0} + \frac{\partial_t c_0}{2c_0}. \quad (22)$$

Moreover if the phase $\phi^\pm$ is solution of the eikonal equation $\mathscr{H}^\pm = 0$, we get by Lemma 2.12

$$\frac{\boldsymbol{w}_g^\pm.\left(\boldsymbol{w}_g^\pm \bar{\otimes} \bar{\bar{\nabla}} \boldsymbol{u}_0 + \boldsymbol{\nabla}_x c_0\right)}{2} = \frac{|\boldsymbol{\nabla}_x \phi^\pm|}{2}\left(\partial_t\left(\frac{1}{|\boldsymbol{\nabla}_x\phi^\pm|}\right) + \boldsymbol{v}_g^\pm.\boldsymbol{\nabla}_x\left(\frac{1}{|\boldsymbol{\nabla}_x\phi^\pm|}\right)\right).$$

We thus replace this result in (22) to obtain

$$< \boldsymbol{e}_{{}^t\Pi^\pm}, L(\boldsymbol{y}, \partial_{\boldsymbol{y}})\boldsymbol{e}_{\Pi^\pm} >= \frac{\mathrm{div}\boldsymbol{v}_g^\pm}{2} + \frac{\rho_0 \boldsymbol{v}_g^\pm}{2c_0|\boldsymbol{\nabla}_x\phi^\pm|^{-1}}.\boldsymbol{\nabla}_{\boldsymbol{x}}\left(\frac{c_0|\boldsymbol{\nabla}_x\phi^\pm|^{-1}}{\rho_0}\right)$$
$$+ \frac{\rho_0}{2c_0|\boldsymbol{\nabla}_x\phi^\pm|^{-1}}\partial_t\left(\frac{c_0|\boldsymbol{\nabla}_x\phi^\pm|^{-1}}{\rho_0}\right).$$

Therefore the equation (19) on $a_0^\pm$ becomes

$$\partial_t a_0^\pm + \boldsymbol{v}_g^\pm.\boldsymbol{\nabla}_{\boldsymbol{x}} a_0^\pm + \frac{1}{2}a_0^\pm \mathrm{div}\boldsymbol{v}_g^\pm$$
$$+ \frac{\rho_0|\boldsymbol{\nabla}_{\boldsymbol{x}}\phi^\pm|}{2c_0}\left(\partial_t\left(\frac{c_0}{\rho_0|\boldsymbol{\nabla}_{\boldsymbol{x}}\phi^\pm|}\right) + \boldsymbol{v}_g^\pm.\boldsymbol{\nabla}_{\boldsymbol{x}}\left(\frac{c_0}{\rho_0|\boldsymbol{\nabla}_{\boldsymbol{x}}\phi^\pm|}\right)\right) = 0.$$

This yields the following conservative equation on $a_0^\pm$

$$\partial_t\left(\frac{a_0^{\pm 2}c_0}{\rho_0|\boldsymbol{\nabla}_x\phi^\pm|}\right) + \mathrm{div}\left(\frac{a_0^{\pm 2}c_0}{\rho_0|\boldsymbol{\nabla}_x\phi^\pm|}\boldsymbol{v}_g^\pm\right) = 0.$$

The equation above is an ODE along the rays. For a regular mean flow, the existence is assured by the classical ODE theory. The uniqueness comes from the fact that transformation $(s, \boldsymbol{\beta}) \longrightarrow \boldsymbol{y}(s, \boldsymbol{\beta})$ is is locally invertible under the transversality condition. □

Remark 2.13. *The above approach holds true for any hyperbolic operator $L(\boldsymbol{y},\partial_y)$ provided that* $\mathrm{Ker}\left(L_1(\boldsymbol{y},\boldsymbol{\nabla}_y\phi)\right)$ *is of dimension one (see [24]). Nevertheless, we must identify geometrically a function v which is solution of the transport equation*

$$\partial_t v + \boldsymbol{v}_g.\boldsymbol{\nabla} v = (\mathrm{div}\boldsymbol{v}_g - 2S)v,$$

with $S =< \boldsymbol{e}_{{}^t\Pi^\pm}, L(\boldsymbol{y},\partial_y)\boldsymbol{e}_{\Pi^\pm} >$. If so, we deduce the conservative transport equation

$$\partial_t\left(\frac{a_0^2}{v}\right) + \mathrm{div}_{\boldsymbol{x}}\left(\frac{a_0^2}{v}\boldsymbol{v}_g\right) = 0.$$

Remark 2.14. *The acoustic perturbation of the velocity field is collinear to the gradient of phase:*

$$\boldsymbol{u}_a = \frac{1}{\rho_0}\boldsymbol{q} - \frac{\varrho}{\rho_0}\boldsymbol{u}_0 = \pm\frac{a_0^\pm c_0}{\rho_0}\frac{\boldsymbol{\nabla}_x\phi^\pm}{|\boldsymbol{\nabla}_x\phi^\pm|}e^{ik\phi^\pm} + O(k^{-1}),$$

i.e. $\boldsymbol{u}_a$ is proportional to the phase velocity $c_0\boldsymbol{w}_g^\pm$.

Corollary 2.15. *For the acoustic modes, the leading term $\mathfrak{p}_0^\pm$ of the asymptotic expansion of the acoustic pressure is solution of the transport equation:*

$$\partial_t\left(\frac{\mathfrak{p}_0^{\pm 2}}{\rho_0 c_0^3|\boldsymbol{\nabla}_x\phi^\pm|}\right) + \mathrm{div}\left(\frac{\mathfrak{p}_0^{\pm 2}}{\rho_0 c_0^3|\boldsymbol{\nabla}_x\phi^\pm|}\boldsymbol{v}_g^\pm\right) = 0. \tag{23}$$

Proof. The linearization of the acoustic pressure is given by:

$$p = \left(c_0^2 - \frac{p_0 s_0}{\rho_0}\right)\varrho + \frac{p_0}{\rho_0}s.$$

Given that the the leading term of asymptotic expansion of the acoustic entropy is given by $d_0^\pm = s_0 a_0^\pm$, $\mathfrak{p}_0^\pm$ is written as a function of the main order term of the asymptotic expansion of the acoustic mass density, *i.e.* $\mathfrak{p}_0^\pm = c_0^2 a_0^\pm$.

The transport equation on $\mathfrak{p}_0^\pm$ is then given by

$$\partial_t\left(\frac{\mathfrak{p}_0^{\pm 2}}{\rho_0 c_0^3|\boldsymbol{\nabla}_x\phi^\pm|}\right) + \mathrm{div}\left(\frac{\mathfrak{p}_0^{\pm 2}}{\rho_0 c_0^3|\boldsymbol{\nabla}_x\phi^\pm|}\boldsymbol{v}_g^\pm\right) = 0.$$

□

3 Computation of the geometrical spreading

In this section, we shall introduce another formulation for the numerical computation of the geometrical optics approximation for the acoustic modes. The source term of the transport equation (17) depends on the second derivatives of the phase through $\mathrm{div}\boldsymbol{v}_g^{\pm}$. Its approximation, by a finite difference method, requires a fairly precise calculation of the phase $\phi^{\pm}$. An alternative approach to this issue is to deduce from (17) a new transport equation where the calculation of $\mathrm{div}\boldsymbol{v}_g^{\pm}$ is replaced with the calculation of a new quantity called *the geometrical spreading*. It is the geometric quantity that measures the evolution of the cross section of an elementary ray tube. This result generalizes, in the case of non-uniform and non-potential mean flow, a well known result for the wave equation [3], and it will be summarized in Proposition 3.4.

3.1 Lagrangian geometrical spreading

The Hamiltonian associated with the acoustic modes is given by

$$\mathscr{H}^{\pm}(t,\boldsymbol{x},\tau,\boldsymbol{\xi}) = \tau + H^{\pm}(\boldsymbol{y},\boldsymbol{\xi}) \quad \text{where} \quad H^{\pm}(\boldsymbol{y},\boldsymbol{\xi}) = \boldsymbol{u}_0(\boldsymbol{y}).\boldsymbol{\xi} \pm c_0(\boldsymbol{y})|\boldsymbol{\xi}|.$$

The Hamiltonian system corresponding to $\mathscr{H}^{\pm}$ is given by

$$\left\{\begin{array}{rcl} \dot{t}(s,\boldsymbol{\beta}) &=& 1 \\ \dot{\boldsymbol{x}}(s,\boldsymbol{\beta}) &=& \mathscr{H}^{\pm}_{\boldsymbol{\xi}}\left(\boldsymbol{y}(s,\boldsymbol{\beta}),\boldsymbol{\eta}(s,\boldsymbol{\beta})\right) \\ \dot{\tau}(s,\boldsymbol{\beta}) &=& -\mathscr{H}^{\pm}_{t}\left(\boldsymbol{y}(s,\boldsymbol{\beta}),\boldsymbol{\eta}(s,\boldsymbol{\beta})\right) \\ \dot{\boldsymbol{\xi}}(s,\boldsymbol{\beta}) &=& -\mathscr{H}^{\pm}_{\boldsymbol{x}}\left(\boldsymbol{y}(s,\boldsymbol{\beta}),\boldsymbol{\eta}(s,\boldsymbol{\beta})\right) \end{array}\right. . \tag{24}$$

Recall that t_0 is the parameter such as $t(s,\boldsymbol{\beta}) = s + t_0$. Note that under the compatibility conditions (**H**.a) and thanks to Proposition 2.9, we have

$$\boldsymbol{\eta}(s,\boldsymbol{\beta}) = \boldsymbol{\nabla}_{\boldsymbol{y}}\phi^{\pm}\left(\boldsymbol{y}(s,\boldsymbol{\beta})\right).$$

Remark 3.1. *We omit from now the index* $\pm$ *in the expression of the bicharacteristics, even if we have a Hamiltonian system associated with each acoustic mode.*

Definition 3.2. ***The lagrangian geometrical spreading*** *is defined as the Jacobian of the ray field with respect to the coordinates of rays, i.e.*

$$J(s,\boldsymbol{\beta}) = \det\left(\partial_s\boldsymbol{y}(s,\boldsymbol{\beta}),\ \partial_{\boldsymbol{\beta}}\boldsymbol{y}(s,\boldsymbol{\beta})\right).$$

Proposition 3.3. *The derivative of the geometrical spreading along the Hamiltonian field is:*

$$\frac{\partial J}{\partial s}(s,\boldsymbol{\beta}) = J(s,\boldsymbol{\beta})\,\mathrm{div}_{\boldsymbol{x}}\boldsymbol{v}_{\boldsymbol{g}}.$$

Proof. Since $t(s,\boldsymbol{\beta})=s+t_0$, the Lagrangian geometrical spreading is:

$$J(s,\boldsymbol{\beta})=\begin{vmatrix} 1 & 1 & {}^t\mathbf{0}_{d-1} \\ \partial_s \boldsymbol{x}(s,\boldsymbol{\beta}) & \partial_{t_0}\boldsymbol{x}(s,\boldsymbol{\beta}) & \partial_{\boldsymbol{\alpha}}\boldsymbol{x}(s,\boldsymbol{\beta}) \end{vmatrix}.$$

Moreover, the derivative of space-time variables with respect to s verifies the differential equation

$$\frac{\partial \boldsymbol{y}}{\partial s}(s,\boldsymbol{\beta})=\begin{pmatrix} 1 \\ \boldsymbol{v_g}\left(\boldsymbol{y}(s,\boldsymbol{\beta})\right) \end{pmatrix},$$

where $\boldsymbol{v_g}\left(\boldsymbol{y}(s,\boldsymbol{\beta})\right)=\mathscr{H}_{\xi}\left(\boldsymbol{y}(s,\boldsymbol{\beta}),\boldsymbol{\nabla}_y\phi\left(\boldsymbol{y}(s,\boldsymbol{\beta})\right)\right)$ is the group velocity.

If we denote by M_J the Jacobian matrix of the transformation between the Lagrangian and the Eulerian coordinates, *i.e.*

$$M_J(s,\boldsymbol{\beta})=\begin{pmatrix} 1 & 1 & {}^t\mathbf{0}_{d-1} \\ \partial_s \boldsymbol{x}(s,\boldsymbol{\beta}) & \partial_{t_0}\boldsymbol{x}(s,\boldsymbol{\beta}) & \partial_{\boldsymbol{\alpha}}\boldsymbol{x}(s,\boldsymbol{\beta}) \end{pmatrix},$$

it follows that its derivative with respect to s writes

$$\frac{\partial M_J}{\partial s}(s,\boldsymbol{\beta})=\begin{pmatrix} 0 & {}^t\mathbf{0}_d \\ \partial_t \boldsymbol{v_g}(\boldsymbol{y}(s,\boldsymbol{\beta})) & \nabla_{\boldsymbol{x}}\boldsymbol{v_g}(\boldsymbol{y}(s,\boldsymbol{\beta})) \end{pmatrix} M_J(s,\boldsymbol{\beta}). \tag{25}$$

Notice that if a matrix M verifies the equation $\frac{\mathrm{d}M}{\mathrm{d}s}(s)=N(s)M(s)$, one gets $\frac{\mathrm{d}}{\mathrm{d}s}(\det M(s))=\mathrm{trace}(N(s))\det M(s)$. We conclude that

$$\frac{\partial J}{\partial s}(s,\boldsymbol{\beta})=J(s,\boldsymbol{\beta})\,\mathrm{div}_{\boldsymbol{x}}\boldsymbol{v_g}.$$

□

By the above, we deduce the following Proposition.

Proposition 3.4. *The quantity* $\dfrac{{a_0}^2 c_0}{\rho_0|\boldsymbol{\nabla}_x\phi|}|J|$ *is conserved along the rays field.*

Proof. If we denote $\mathfrak{C}=\dfrac{{a_0}^2 c_0}{\rho_0|\boldsymbol{\nabla}_x\phi|}$, we check that

$$\frac{\partial}{\partial s}\left(\mathfrak{C}(\boldsymbol{y}(s,\boldsymbol{\beta}))\left|J(s,\boldsymbol{\beta})\right|\right)= \left|J(s,\boldsymbol{\beta})\right|\left(\frac{\partial \mathfrak{C}}{\partial s}(\boldsymbol{y}(s,\boldsymbol{\beta}))+\frac{\mathfrak{C}(\boldsymbol{y}(s,\boldsymbol{\beta}))}{\left|J(s,\boldsymbol{\beta})\right|}\frac{\partial |J|}{\partial s}(s,\boldsymbol{\beta})\right).$$

Thanks to the equation (17) and Proposition 3.3, it follows that

$$\left(\partial_t \mathfrak{C} + \boldsymbol{v}_g.\boldsymbol{\nabla}_x \mathfrak{C}\right)\left|J(s,\boldsymbol{\beta})\right| + \mathrm{div}(\boldsymbol{v}_g)\left|J(s,\boldsymbol{\beta})\right|\mathfrak{C}(\boldsymbol{y}(s,\boldsymbol{\beta})) = 0,$$

which gives the result. □

This generalizes the classical result for the wave equation (which is the conservation of the product of the energy and the geometrical spreading along the rays).

Finally, we have demonstrated that the quantity $\mathfrak{C}|J|$ is constant along the ray field. The calculation of the geometrical optics term turns therefore to the calculation of the geometrical spreading J and the function $\mathfrak{C}$. The calculation of J is equivalent to the calculation of $\partial_{\boldsymbol{\beta}}\boldsymbol{x}$. Indeed, the quantities $\partial_s \boldsymbol{x}$ are given directly by $H_\xi(\boldsymbol{y}, \boldsymbol{\nabla}_x \phi)$. This is made possible by the calculation of the phase ϕ (first step of our numerical part).

Derivating with respect to $\boldsymbol{\beta}$ the Hamiltonian system associated with $\mathscr{H}$, we obtain a transport equation for the derivative of the bicharacteristic with respect to the parameterization of the incident surface Σ_{inc}, *i.e.*

$$\frac{\partial}{\partial s}\begin{pmatrix} \partial_{\boldsymbol{\beta}}\boldsymbol{y}(s,\boldsymbol{\beta}) \\ \partial_{\boldsymbol{\beta}}\boldsymbol{\eta}(s,\boldsymbol{\beta}) \end{pmatrix} = \begin{pmatrix} \mathscr{H}_{y\eta}(\boldsymbol{y},\boldsymbol{\eta}) & \mathscr{H}_{\eta\eta}(\boldsymbol{y},\boldsymbol{\eta}) \\ -\mathscr{H}_{yy}(\boldsymbol{y},\boldsymbol{\eta}) & -\mathscr{H}_{\eta y}(\boldsymbol{y},\boldsymbol{\eta}) \end{pmatrix}\begin{pmatrix} \partial_{\boldsymbol{\beta}}\boldsymbol{y}(s,\boldsymbol{\beta}) \\ \partial_{\boldsymbol{\beta}}\boldsymbol{\eta}(s,\boldsymbol{\beta}) \end{pmatrix}, \tag{26}$$

with the initial condition

$$\begin{pmatrix} \partial_{\boldsymbol{\beta}}\boldsymbol{y}(0,\boldsymbol{\beta}) \\ \partial_{\boldsymbol{\beta}}\boldsymbol{\eta}(0,\boldsymbol{\beta}) \end{pmatrix} = \begin{pmatrix} \partial_{\boldsymbol{\beta}}\mathbf{y}_0(\boldsymbol{\beta}) \\ \partial_{\boldsymbol{\beta}}\boldsymbol{\eta}_0(\boldsymbol{\beta}) \end{pmatrix}, \tag{27}$$

where η_0 verifies the compatibility condition with the Lagrangian incident phase φ_{inc}. We can consider any incident wave (and not only a plane wave) and the point $(\boldsymbol{y},\boldsymbol{\eta})$ is in the asymptotic wave front set of this incident wave.

Remark 3.5. *Unlike the equation (25), the equation (26) will involve just the first derivatives of the phase.*

3.2 Eulerian geometrical spreading

In this section, we will calculate the quantity, that we called the geometrical spreading, in the neighborhood of any point not belonging to a caustic. In presence of a caustic, there exists N local diffeomorphisms between each point y (not belonging to the caustic) and the associated Lagrangian coordinates $\left(s_p, \boldsymbol{\beta}_p\right)_{1\leq p\leq N}$ where $\boldsymbol{y}$ has N antecedents by the application $\boldsymbol{y} = \boldsymbol{y}(s,\boldsymbol{\beta})$. Hence,

for simplicity, we will place ourselves in the framework where rays do not cross. The generalisation to the previous situation is straightforward.

Let be $\mathscr{Y}_0$ the Eulerian function which gives the initial time t_0 and the initial position $\boldsymbol{\alpha}$ on the surface Γ_{inc}, of the ray that passes through the point $\boldsymbol{x}$ at time t, and the function $\mathscr{S}_0$ which gives the curvilinear abscissa on the ray, *i.e.*

$$\Big(\mathscr{S}_0\left(t(s,\boldsymbol{\beta}),\boldsymbol{x}(s,\boldsymbol{\beta})\right),\mathscr{Y}_0(t(s,\boldsymbol{\beta}),\boldsymbol{x}(s,\boldsymbol{\beta}))\Big)\equiv\Big(s,\boldsymbol{\beta}\Big).$$

We can thus define, from the Lagrangian quantities, the corresponding Eulerian ones as follows

$$U(t,\boldsymbol{x})=\begin{pmatrix}\boldsymbol{\Theta}(t,\boldsymbol{x})\\ \boldsymbol{\Lambda}(t,\boldsymbol{x})\end{pmatrix}=\begin{pmatrix}\partial_{\boldsymbol{\beta}}\boldsymbol{y}\left(\mathscr{S}_0(t,\boldsymbol{x}),\mathscr{Y}_0(t,\boldsymbol{x})\right)\\ \partial_{\boldsymbol{\beta}}\boldsymbol{\eta}\left(\mathscr{S}_0(t,\boldsymbol{x}),\mathscr{Y}_0(t,\boldsymbol{x})\right)\end{pmatrix},\tag{28}$$

which is a matrix of order $(2(d+1))\times(d+1)$. This matrix will be called, in the sequel, **the stretching matrix**, because it shows the stretching of the rays.

The **Eulerian geometrical spreading** G is defined by

$$G(t,\boldsymbol{x})=J\left(\mathscr{S}_0(t,\boldsymbol{x}),\mathscr{Y}_0(t,\boldsymbol{x})\right).$$

Proposition 3.6. *For the acoustic modes, the computation of the leading term of the asymptotic expansion is done through:*

❶ *the function U solution of the transport equation*

$$\partial_t U(t,\boldsymbol{x})+\boldsymbol{v}_g.\nabla_{\boldsymbol{x}}U(t,\boldsymbol{x})=\mathscr{M}(\boldsymbol{x},\boldsymbol{\nabla}_{\boldsymbol{x}}\phi)U(t,\boldsymbol{x}),\tag{29}$$

The matrix $\mathscr{M}$ is given by the derivatives of the Hamiltonian with respect to the coordinates in the phase space, i.e.

$$\mathscr{M}(\boldsymbol{y},\boldsymbol{\nabla}_{\boldsymbol{y}}\phi)=\begin{pmatrix}\mathscr{H}_{\boldsymbol{y}\boldsymbol{\eta}}(\boldsymbol{y},\boldsymbol{\nabla}_{\boldsymbol{y}}\phi) & \mathscr{H}_{\boldsymbol{\eta}\boldsymbol{\eta}}(\boldsymbol{y},\boldsymbol{\nabla}_{\boldsymbol{y}}\phi)\\ -\mathscr{H}_{\boldsymbol{y}\boldsymbol{y}}(\boldsymbol{y},\boldsymbol{\nabla}_{\boldsymbol{y}}\phi) & -\mathscr{H}_{\boldsymbol{\eta}\boldsymbol{y}}(\boldsymbol{y},\boldsymbol{\nabla}_{\boldsymbol{y}}\phi)\end{pmatrix}.$$

❷ *the function $\mathscr{C}=\dfrac{{a_0}^2c_0G}{\rho_0|\boldsymbol{\nabla}_{\boldsymbol{x}}\phi^{\pm}|}$ solution of the transport equation:*

$$\partial_t\mathscr{C}(t,\boldsymbol{x})+\boldsymbol{v}_g.\boldsymbol{\nabla}_{\boldsymbol{x}}\mathscr{C}=0.\tag{30}$$

The incident condition on U is given by (27) and by φ_{inc} and a_{inc} for $\mathscr{C}$.

Proof. By combining (28) and (26), we get the derivative of the function U along the rays field:

$$\frac{\partial}{\partial s}\left(U(\boldsymbol{y}(s,\boldsymbol{\beta}))\right)=\mathscr{M}\left(\boldsymbol{y}(s,\boldsymbol{\beta}),\boldsymbol{\nabla}_{\boldsymbol{x}}\phi(\boldsymbol{y}(s,\boldsymbol{\beta}))\right)U\left(\boldsymbol{y}(s,\boldsymbol{\beta})\right).$$

On the other hand, we have

$$\frac{\partial \boldsymbol{y}}{\partial s}(s,\boldsymbol{\beta})=\frac{\partial}{\partial s}\begin{pmatrix} t(s,\boldsymbol{\beta}) \\ \boldsymbol{x}(s,\boldsymbol{\beta}) \end{pmatrix}=\begin{pmatrix} 1 \\ \boldsymbol{v}_g\left(\boldsymbol{y}(s,\boldsymbol{\beta}),\boldsymbol{\eta}(s,\boldsymbol{\beta})\right) \end{pmatrix},$$

which leads to (29) thanks to $\boldsymbol{\eta}(s,\boldsymbol{\beta})=\boldsymbol{\nabla}_{\boldsymbol{y}}\phi(\boldsymbol{y}(s,\boldsymbol{\beta}))$ (by Proposition 2.9), and having $v_i=H_{\xi_i}$.

It remains to establish the equation on $\mathscr{C}$. Owing to Proposition 3.4, the material derivative of $\mathscr{C}$ along the rays field is zero, *i.e.*

$$\partial_t\mathscr{C}(t,\boldsymbol{x})+\sum_{i=1}^{d}H_{\xi_i}(\boldsymbol{x},\boldsymbol{\nabla}_{\boldsymbol{x}}\phi)\partial_{x_i}\mathscr{C}(t,\boldsymbol{x})=0,$$

or still $$\partial_t\mathscr{C}(t,\boldsymbol{x})+\boldsymbol{v}_g(t,\boldsymbol{x}).\boldsymbol{\nabla}_{\boldsymbol{x}}\mathscr{C}(t,\boldsymbol{x})=0.$$ □

4 Numerical scheme for the eikonal equation

We apply in this paper a numerical Eulerian method to calculate the solution of the eikonal equations associated to the acoustic modes. This approach to determine an approximation of the solution of Hamilton-Jacobi equations has been used in several areas of applications, such as in electromagnetic in the high frequency regime (see Benamou *et al.* [2]), the shape-from-shading problem (see Lions, Rouy, Tourin [34]), and optimal control (Crandall, Lions [7]). Note that it differs from the usual ray method, which consists in solving ordinary differential equations for unknowns along a Lagrangian trajectory. The advantage of the method used here is that we compute the phase ϕ on a fixed Eulerian grid.

We use a finite difference type methods and more precisely a class of monotone schemes, investigated by Crandall and Lions [7], based upon a numerical Hamiltonian. The numerical solutions calculated through monotone schemes converge to a viscosity solution which belongs to a class of weak solutions of Hamilton-Jacobi equations characterized by entropy inequalities (Barles [1]).

This viscosity solution selects (when the phase is multivalued) what the geophysicists call usually the first-arrival travel time:

$$\phi(\boldsymbol{y}) = \min_{\{(s,\boldsymbol{\beta})/\boldsymbol{y}=\boldsymbol{y}(s,\boldsymbol{\beta})\}} \varphi(s,\boldsymbol{\beta}),$$

where φ is the Lagrangian phase solution of (13) with $\varphi_{|_{\Sigma_{inc}}} = \varphi_{inc}$.

4.1 First order Eulerian numerical scheme

We consider the eikonal equations for the acoustics modes, *i.e.*

$$\partial_t \phi + H^{\pm}(x,y,\partial_x\phi,\partial_y\phi) = 0, \tag{31}$$

where $H^{\pm}(x,y,\xi,\zeta) = u_0(x,y)\xi + v_0(x,y)\zeta \pm c_0(x,y)\sqrt{\xi^2+\zeta^2}$ is a convex (*resp.* concave) function with respect to ξ and ζ for the acoustic mode + (*resp.* -).

Remark 4.1. *Throughout this study, unless otherwise stated, we will give the incident condition, on the incident surface*

$$\Sigma_{inc} \equiv \mathbb{R} \times \Gamma_{inc}, \;\; \textit{where}\, \Gamma_{inc} = \{(0,y_0);\; y_0 \in [y_{min}, y_{max}] \subset \mathbb{R}\},$$

by the trace of the analytical solutions that will be calculated. We present the various experiments carried out for which we have obtained the analytical solutions, which here allowed us to test the validity of our numerical schemes.

To solve the equation (31), we define a uniform mesh of the rectangular domain $\Omega \equiv [x_{min}, x_{max}] \times [y_{min}, y_{max}]$ where $\triangle x$ and $\triangle y$ are the grid spacings and $\triangle t$ is the time step that should satisfy the C.F.L. condition that will be given later. Let $\phi^n_{i,j}$ denote a numerical approximation to the viscosity solution $\phi^n_{i,j} = \phi(t_n, x_i, y_j)$ at the grid point $(i\triangle x, j\triangle j)$ and at the discrete time $n\triangle t$.

The upwind derivative operators are:

$$u_l = D^-_x \phi^n_{i,j} = \frac{\phi^n_{i,j} - \phi^n_{i-1,j}}{\triangle x} \quad , \quad u_r = D^+_x \phi^n_{i,j} = \frac{\phi^n_{i+1,j} - \phi^n_{i,j}}{\triangle x}$$

$$v_l = D^-_y \phi^n_{i,j} = \frac{\phi^n_{i,j} - \phi^n_{i,j-1}}{\triangle y} \quad , \quad v_r = D^+_y \phi^n_{i,j} = \frac{\phi^n_{i,j+1} - \phi^n_{i,j}}{\triangle y}.$$

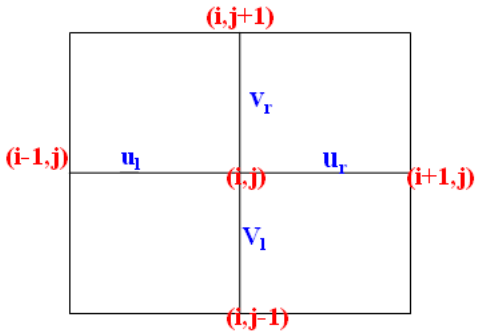

Figure 1: Stencil of upwind scheme around the vertex $(i\triangle x, j\triangle y)$.

We use a five point explicit finite difference scheme:

$$\phi_{i,j}^{n+1} = \phi_{i,j}^{n} - \triangle t \hat{H}^{\pm}(t_n, x_i, y_j, u_l, u_r, v_l, v_r), \tag{32}$$

where $\hat{H}^{\pm}$ is the numerical Hamiltonian associated with the Hamiltonian $H^{\pm}$.

Crandall and Lions [7], and thereafter Souganidis [40] have proved the convergence of the monotone scheme, for Hamilton-Jacobi equations, to the viscosity solution. In [34], Osher and Shu have given the conditions on the numerical Hamiltonian, which ensures the stability and convergence of the numerical scheme:

Hypothesis:
(**H**.1) $\hat{H}$ is a continuous function in all its variables and Lipschitz in the dual variables (u_l, u_r, v_l, v_r).
(**H**.2) $\hat{H}$ is consistent with the Hamiltonian H: $\hat{H}(u,u,v,v) = H(u,v)$.
(**H**.3) $\hat{H}$ is monotone, in the sense that it is an increasing function with respect to its first and third variables and decreasing with respect to its second and fourth variables. Schematically we have $\hat{H}(\uparrow,\downarrow,\uparrow,\downarrow)$.

Under these conditions, we have the convergence of the numerical scheme to the viscosity solution (see [34]):

$$\|\phi_{visc}(t_n, x_i, y_j) - \phi_{i,j}^{n}\|_{L^\infty} \leq C\sqrt{\triangle t},$$

where C is a positive constant independent of the time step.

The numerical Hamiltonian proposed in this paper to solve the equation (31) is basically a modification of the numerical Hamiltonian of Godunov. Indeed, the Hamiltonian H^+ (*resp.* H^-) is composed of a convex (*resp.* concave)

part and a part convected by the mean flow. We are approximating the convex or the concave part by the numerical Hamiltonian of Godunov and the convected part by the upwind scheme in the direction of the mean flow field through:

$$\begin{aligned}\hat{H}^{\epsilon}(x,y,u_l,u_r,v_l,v_r) = u_0^+(x,y)u_l - u_0^-(x,y)u_r \\ + v_0^+(x,y)v_l - v_0^-(x,y)v_r + F^{\epsilon}(x,y,u_l,u_r,v_l,v_r),\end{aligned} \quad (33)$$

with $$\begin{cases} F^+(x,y,u_l,u_r,v_l,v_r) &= c_0(x,y)\sqrt{\max^2(u_l^+,u_r^-)+\max^2(v_l^+,v_r^-)} \\ F^-(x,y,u_l,u_r,v_l,v_r) &= - c_0(x,y)\sqrt{\max^2(u_l^-,u_r^+)+\max^2(v_l^-,v_r^+)} \end{cases}.$$

For $x \in \mathbb{R}$, we denoted by $x^+ = \max(x,0)$ and $x^- = \max(-x,0)$. We recall that the numerical Hamiltonian of Godunov is giving by:

$$\hat{H}_G(x,y,u_l,u_r,v_l,v_r) = \operatorname*{ext}_{v\in I(v_l,v_r)} \operatorname*{ext}_{u\in I(u_l,u_r)} H(x,y,u,v),$$

where $I(a,b) = [\min(a,b),\max(a,b)] \subset \mathbb{R}$ and $\operatorname{ext} = \begin{cases} \min\limits_{a\le u\le b} & \text{if} \quad a \le b, \\ \max\limits_{b\le u\le a} & \text{if} \quad a > b \end{cases}.$

Proposition 4.2. *Assume that the mean flow is regular, the numerical Hamiltonian (33) verifies the hypothesis (***H***.1)-(***H***.2), and the hypothesis (***H***.3) under the C.F.L. condition:*

$$\frac{\triangle t}{\triangle x}\|u_0\|_\infty + \frac{\triangle t}{\triangle y}\|v_0\|_\infty + \left(\frac{\triangle t}{\triangle x} + \frac{\triangle t}{\triangle y}\right)\|c_0\|_\infty \le 1. \quad (34)$$

Proof. For the sake of brevity, the proof is done just for the numerical Hamiltonian $\hat{H}^+$, and that for $\hat{H}^-$ can be made in the same way. We shall prove that $\hat{H}^+$ is a Lipschitz function in the dual variables, and after we shall discuss its monotonicity.

▷ ***Proof of Lipschitzity.*** We consider $(u_{l_1},u_{r_1},v_{l_1},v_{r_1})$ and $(u_{l_2},u_{r_2},v_{l_2},v_{r_2})$ on $\mathbb{R}^4$. We have the inequality

$$(\max(u_{l_1}^+,u_{r_1}^-) - \max(u_{l_2}^+,u_{r_2}^-))^2 \le (u_{l_1}-u_{l_2})^2 + (u_{r_1}-u_{r_2})^2.$$

For proving that, we may study separately the two following cases:

• **Case 1:** $\begin{cases} \max(u_{l_1}^+,u_{r_1}^-) = u_{l_1} \\ \max(u_{l_2}^+,u_{r_2}^-) = u_{l_2} \end{cases}$ or $\begin{cases} \max(u_{l_1}^+,u_{r_1}^-) = -u_{r_1} \\ \max(u_{l_2}^+,u_{r_2}^-) = -u_{r_2} \end{cases}$,

• **Case 2:** $\left\{\begin{array}{rcl}\max(u_{l_1}^+,u_{r_1}^-) &=& u_{l_1}\\ \max(u_{l_2}^+,u_{r_2}^-) &=& -u_{r_2}\end{array}\right.$ or $\left\{\begin{array}{rcl}\max(u_{l_1}^+,u_{r_1}^-) &=& -u_{r_1}\\ \max(u_{l_2}^+,u_{r_2}^-) &=& u_{l_2}\end{array}\right.$,

We then show the inequality

$$\left|\hat{H}^+(u_{l_1},u_{r_1},v_{l_1},v_{r_1})-\hat{H}^+(u_{l_2},u_{r_2},v_{l_2},v_{r_2})\right| \\ \leq \lambda\left|\left|(u_{l_1},u_{r_1},v_{l_1},v_{r_1})-(u_{l_2},u_{r_2},v_{l_2},v_{r_2})\right|\right|_{\mathbb{R}^4},$$

where $\lambda = 3\max(||u_0||_\infty, ||v_0||_\infty, ||c_0||_\infty)$. ◁

▷ ***Proof of monotonicity.*** The numerical scheme (32) can be written as:

$$\phi_{i,j}^{n+1} = \hat{G}^+(\phi_{i,j}^n, \phi_{i+1,j}^n, \phi_{i,j+1}^n, \phi_{i-1,j}^n, \phi_{i,j-1}^n).$$

The numerical scheme is monotone if the function $\hat{G}^+$ is increasing with respect to each of its variables. The monotonicity with respect to $\phi_{i-1,j}^n$ and $\phi_{i,j-1}^n$ is equivalent to show that $\hat{H}$ is increasing with respect to u_l and v_l, and it is decreasing with respect to u_r and v_r for the monotony with respect to $\phi_{i,j+1}^n$ and $\phi_{i+1,j}^n$.

One can show that $\hat{G}^+$ is unconditionally monotone with respect to $\phi_{i\pm1,j}^n$ and $\phi_{i,j\pm1}^n$. It remains to give the condition which ensures the monotonicity of $\hat{G}^+$ with respect to $\phi_{i,j}^n$. We have

$$\frac{\partial \hat{G}^+}{\partial \phi_{i,j}^n} = 1-\triangle t\left[\frac{u_0^+ + u_0^-}{\triangle x}+\frac{v_0^+ + v_0^-}{\triangle y}+c_0\left(\frac{\max(u_l^+,u_r^-)}{\triangle x\sqrt{\max^2(u_l^+,u_r^-)+\max^2(v_l^+,v_r^-)}}\right.\right. \\ \left.\left.+\frac{\max(v_l^+,v_r^-)}{\triangle y\sqrt{\max^2(u_l^+,u_r^-)+\max^2(v_l^+,v_r^-)}}\right)\right].$$

Since $|x| = x^+ + x^-$, it follows that

$$\frac{\partial \hat{G}^+}{\partial \phi_{i,j}^n} = 1-\triangle t\left[\frac{|u_0|}{\triangle x}+\frac{|v_0|}{\triangle y}+c_0\left(\frac{\max(u_l^+,u_r^-)}{\triangle x\sqrt{\max^2(u_l^+,u_r^-)+\max^2(v_l^+,v_r^-)}}\right.\right. \\ \left.\left.+\frac{\max(v_l^+,v_r^-)}{\triangle y\sqrt{\max^2(u_l^+,u_r^-)+\max^2(v_l^+,v_r^-)}}\right)\right].$$

It ensues that under the condition

$$\frac{\triangle t}{\triangle x}||u_0||_\infty+\frac{\triangle t}{\triangle y}||v_0||_\infty+\left(\frac{\triangle t}{\triangle x}+\frac{\triangle t}{\triangle y}\right)||c_0||_\infty \leq 1,$$

the numerical Hamiltonian $\hat{H}^+$ is monotone with respect to $\phi^n_{i,j}$. ◁

One can easily verify that the numerical Hamiltonian $\hat{H}^+$ is consistent with the Hamiltonian H^+ and it is continuous. In conclusion, the numerical Hamiltonian $\hat{H}^+$ satisfies the assumptions given by Osher and Shu [34]. Thus, the numerical scheme (32) converges to the viscosity solution of the eikonal equation(31). □

4.2 Analytical boundary conditions

We recall here a basic test case (studied previously in [33]). We consider a two-dimensional homogeneous medium ($c_0 \equiv 1$) with a shear mean flow (*i.e.* flow with zero vertical component $v_0 \equiv 0$ and depending only on the transverse coordinate):

$$u_0(y) = M_0 + M_0' y.$$

The incident wave is a wave whose trace of the gradient of the phase on the incidente surface $\Gamma_{inc} = \{(0, y_0)\}$ is given by $(\cos\alpha, \sin\alpha)$, $\alpha \in [0, \pi/2[$ (no grazing ray).

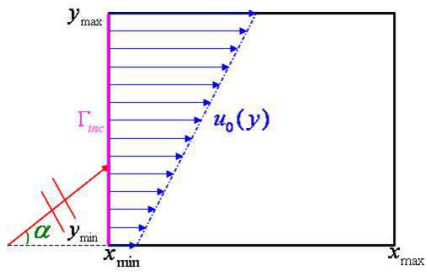

Figure 2: Shear flow, incident plane wave.

The analytical solution, for the eikonal equation associated to the acoustic mode +, is (see [32]):

$$\begin{aligned}\phi(t,x,y) = {} & x\cos\alpha + y\sin\alpha - u_0(y)t\cos\alpha \\ & + \frac{\sin\alpha - M_0' t\cos\alpha}{2M_0'\cos\alpha}\sqrt{\cos^2\alpha + (\sin\alpha - M_0' t\cos\alpha)^2} \\ & - \frac{\cos\alpha}{2M_0'}\ln\left(\sqrt{\cos^2\alpha + (\sin\alpha - M_0' t\cos\alpha)^2} - (\sin\alpha - M_0' t\cos\alpha)\right), \quad (35)\end{aligned}$$

with the initial condition

$$\phi_0(x,y) = x\cos\alpha + y\sin\alpha + \frac{1}{2M_0'}\Big(\tan\alpha - \cos\alpha\ln(1-\sin\alpha)\Big). \tag{36}$$

Remark 4.3.
• *In the case of shear flow with $c_0 \equiv 1$, we note that we have uniqueness of the viscosity solution of the Hamilton-Jacobi equation $\mathscr{H}^+ = 0$ in $\mathbb{R}^2$ with the iniital condition (36) (see Barles [1]), thanks to the inequality:*

$$\Big|H^+(x_1,y_1,\xi,\zeta) - H^+(x_2,y_2,\xi,\zeta)\Big| \le |M_0'|\left(1+\sqrt{\xi^2+\zeta^2}\right)|y_1-y_2|.$$

• *In the case of a static inhomogeneous medium (test cases developed later), i.e. $u_0 = v_0 = 0$ and c_0 is not constant, we have also the uniqueness of the viscosity solution of the equation $\mathscr{H}^+ = 0$ in $\mathbb{R}^2$ together with a smooth initial condition under the hypothesis that c_0 is is continuous with bounded derivatives, thanks to the iniquality:*

$$\Big|H^+(x_1,y_1,\xi,\zeta) - H^+(x_2,y_2,\xi,\zeta)\Big| \le L\left(1+\sqrt{\xi^2+\zeta^2}\right)\Big|\Big|(x_1,y_1)-(x_2,y_2)\Big|\Big|_{\mathbb{R}^2},$$

where L is a positive constant such that $||\boldsymbol{\nabla} c_0||_{L^\infty} \le L$.

The ray field is given by:

$$\begin{cases} x(s,y_0) = & \left(u_0(y_0) + \dfrac{1}{\cos\alpha}\right)s + \dfrac{\sin\alpha - M_0' s\cos\alpha}{2M_0'\cos^2\alpha}\sqrt{\cos^2\alpha + (\sin\alpha - M_0' s\cos\alpha)^2} \\ & -\dfrac{1}{2M_0'}\ln\left(\sin\alpha - M_0' s\cos\alpha + \sqrt{\cos^2\alpha + (\sin\alpha - M_0' s\cos\alpha)^2}\right) \\ & +\dfrac{1}{2M_0'}\ln(\sin\alpha+1) - \dfrac{\sin\alpha}{2M_0'\cos^2\alpha}, \\ y(s,y_0) = & \dfrac{1}{M_0'\cos\alpha}\left(1 - \sqrt{\cos^2\alpha + (\sin\alpha - M_0' s\cos\alpha)^2}\right) + y_0. \end{cases} \tag{37}$$

Remark 4.4. *Along the ray field, the horizontal component of the group velocity vanishes at $s = M_0'\tan\alpha$, then there is a y_{max} such that $y(s,y_0) \le y_{max}$ for all s. For an initial position $y_0 \in \Gamma_{inc}$ and an angle of incidence α, the point y_{max} is given by:*

$$y_{max}(y_0,\alpha) = \frac{1-\cos\alpha}{M_0'\cos\alpha} + y_0.$$

This phenomenon is well known in acoustic propagation in the atmosphere [5]. Under the effect of shear flow, the rays are deflected and can not exceed a maximum ordinate y_{max}. This is illustrated by the next paragraph.

We test firstly the first order interior scheme. For this, the unknown function ϕ is given in the whole boundary of $\Omega =]0,1[\times]0,1[$ by the Dirichlet condition obtained as the trace of the analytic phase (35). We have verified the mesh convergence for two test cases. The error in the L^∞ norm between the numerical and analytical solutions of the eikonal equation (associated to the acoustic mode +) is shown in table 1. It put in evidence an experimental convergence order of 0.96 and 1.02 for the test case $\boldsymbol{u_0(y) = 0.3 + 0.2y, \alpha = \pi/6}$ and the test case $\boldsymbol{u_0(y) = 0.1 + 0.4y, \alpha = \pi/7}$ respectively.

$\boldsymbol{u_0(y) = 0.3 + 0.2y, \alpha = \pi/6}$		
Mesh	Iterations	Error L^∞
50×50	5000	0.001478
100×100	10000	0.00074
150×150	15000	0.00050
200×200	20000	0.00037
250×250	25000	0.000298
300×300	30000	0.000248]
E.C.O = 0.96		

$\boldsymbol{u_0(y) = 0.1 + 0.4y, \alpha = \pi/7}$		
Mesh	Iterations	Error L^∞
50×50	5000	0.0032
100×100	10000	0.0016
150×150	15000	0.0010
200×200	20000	0.0008
250×200	25000	0.0006
300×200	30000	0.0005
E.C.O = 1.02		

Table 1: Error in L^∞ norm at fixed time.

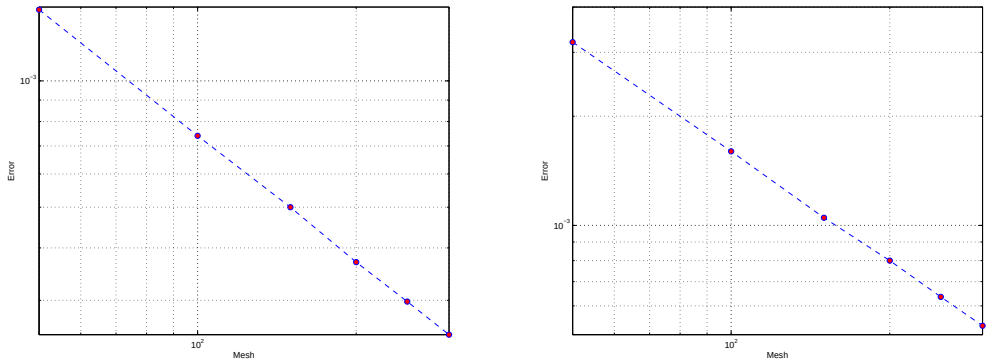

Figure 3: Evolution of the error L^∞ in logarithmic scale.

4.3 Parametric study for a shear flow

■ Influence of the parameters of the shear flow

E.C.O. denotes the Experimental Convergence Order

In what follows, we represent the countour lines of the phase ϕ (given by the numerical scheme) and the ray tracing (given by the analytical expression (37)) for different values of the parameters of the shear flow and for $\alpha = \frac{\pi}{6}$.

▮ $u_0(y) = 0.5$ **(uniform mean flow)**

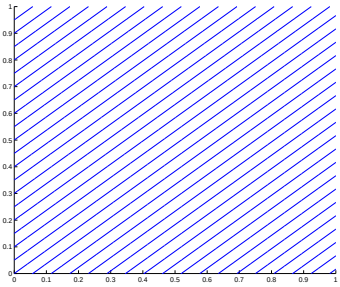

Figure 4: Ray tracing

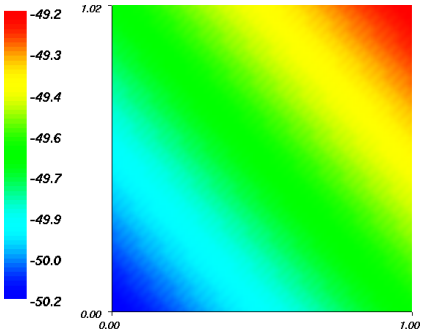

Countour lines at $t = 1.5s$.

▮ $u_0(y) = 0.6y$

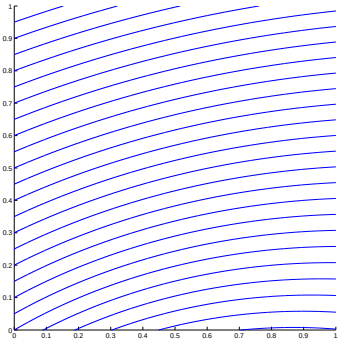

Figure 5: Ray tracing

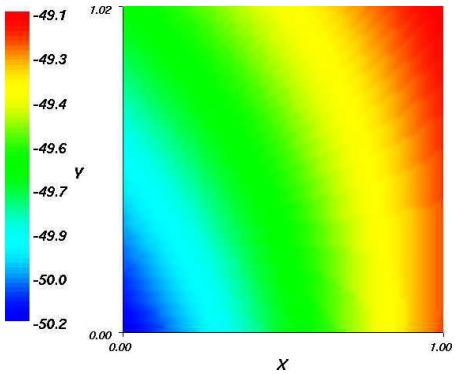

Countour lines at $t = 1.5s$.

▮ $u_0(y) = -0.5 + 0.6y$

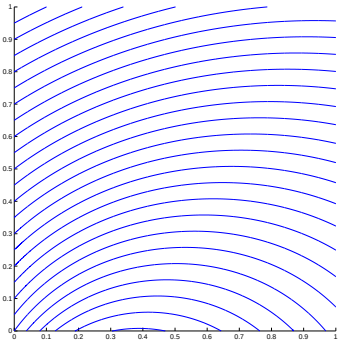

Figure 6: Ray tracing

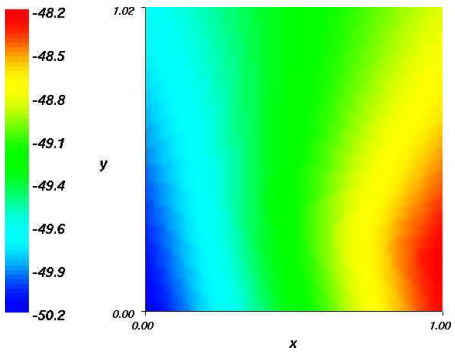

Countour lines at $t = 1.5s$.

■ Influence of the incidence angle

We set the following mean flow profile: $\boldsymbol{u}_0(y) = 0.6y$, and we look at the influence of the angle of incidence.

▮ $\alpha = 0°$

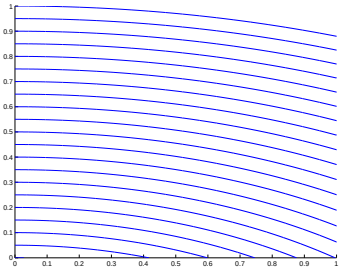

Figure 7: Ray tracing

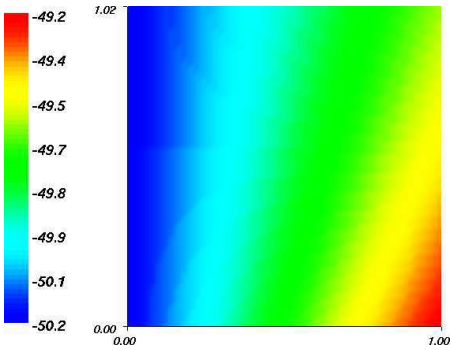

Countour lines at $t = 1.5s$.

▮ $\alpha = 40°$

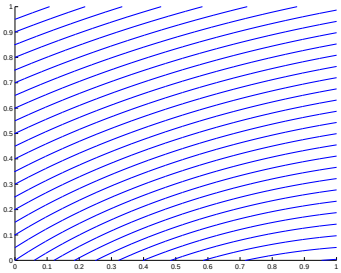

Figure 8: Ray tracing

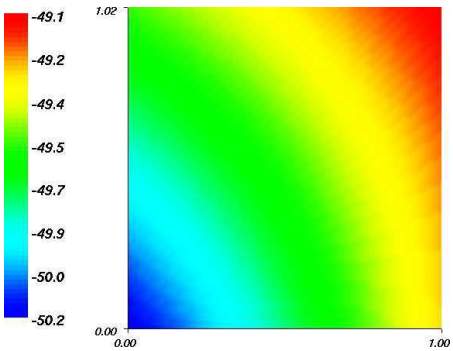

Countour lines t at $t = 1.5s$.

▮ $\theta = 60°$

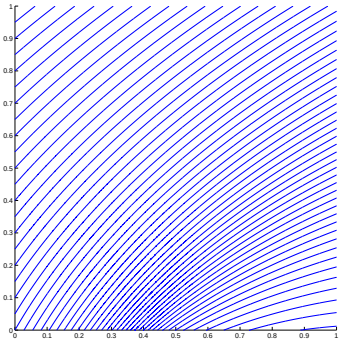

Figure 9: Ray tracing

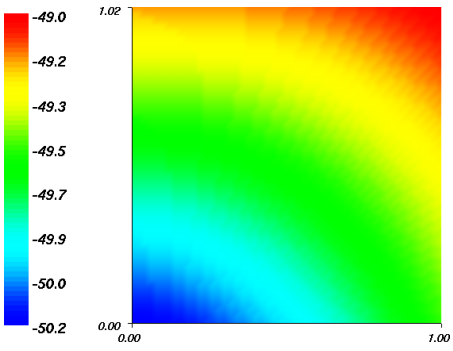

Countour lines at $t = 1.5s$.

4.4 Numerical boundary conditions

The previous results have validated the interior scheme. It remains to deal with the scheme at the boundaries of the computational domain. Recall that the eikonal equation is equivalent to an advection equation along the group velocity $\boldsymbol{v}_g^{\pm}$. Indeed, we have:

$$\partial_t \phi^{\pm} + \boldsymbol{u}_0(\boldsymbol{x}).\boldsymbol{\nabla}_{\boldsymbol{x}}\phi^{\pm} \pm c_0(\boldsymbol{x})|\boldsymbol{\nabla}_{\boldsymbol{x}}\phi^{\pm}| = \partial_t \phi^{\pm} + \underbrace{\left(\boldsymbol{u}_0(\boldsymbol{x}) \pm c_0(\boldsymbol{x})\frac{\boldsymbol{\nabla}_{\boldsymbol{x}}\phi^{\pm}}{|\boldsymbol{\nabla}_{\boldsymbol{x}}\phi^{\pm}|}\right)}_{\boldsymbol{v}_g^{\pm}}.\boldsymbol{\nabla}_{\boldsymbol{x}}\phi^{\pm} = 0.$$

By the interpretation with the characteristics, we need a given Dirichlet condition on incoming boundaries Γ_{in} (part of the boundary on which we have $\boldsymbol{v}_g.\boldsymbol{n} < 0$ where $\boldsymbol{n}$ is the outward normal vector to Γ_{in}). The incoming conditions can be thought of as originating from a problem on a larger spatial domain.

The main goal will be to take into account the outgoing conditions. Two cases arise: the case of an artificial boundary and the case of a physical boundary. In the latter, one may generate reflected rays. We shall not consider this case in the present paper. Our study concentrates on an artificial boundary with outgoing condition.

In this subsection, we will present two approaches for the implementation of the outgoing boundary conditions. Physically speaking, the rays are going outside the domain Ω of the study without reflection. We will investigate the following approaches:

(a) The first approach is based on an extrapolation of the values of the phase on the boundary by its neighboring cells values (*e.g.* [2]).

(b) The second approach is to adapt the interior scheme at the boundaries.

- **Outgoing boundary conditions by extrapolation**

On the edges $x_{max} = I \triangle x$, $y_{min} = 0$, and $y_{max} = J \triangle y$, we assume that the rays are outgoing. The approach consists in adding fictitious points outside the boundary on which the phase is calculated by extrapolation:

$$\phi_{I+1,j}^{n+1} = 2\phi_{I,j}^{n+1} - \phi_{I-1,j}^{n+1}, \quad j \in [\![0, J+1]\!],$$

on the fictitious edges 0 and $J+1$, we proceed in the same way:

$$\phi_{i,J+1}^{n+1} = 2\phi_{i,J}^{n+1} - \phi_{i,J-1}^{n+1}, \quad i \in [\![1, I+1]\!],$$

$$\phi_{i,0}^{n+1} = 2\phi_{i,1}^{n+1} - \phi_{i,2}^{n+1}, \quad i \in [\![1, I+1]\!].$$

The following table gives the L^∞ error, on the mesh points, between the numerical phase and the analytical one (previously calculated for $u_0(y) = 0.1 + 0.3y$ and $\alpha = \frac{\pi}{4}$) at time $t = 50s$, and the figure shows the mesh convergence with a logarithmic scale.

$u_0(y) = 0.1 + 0.3y, \alpha = \pi/4$		
Mesh	Iterations	Error L^∞
10×10	1000	0.007366
20×20	2000	0.003733
30×30	3000	0.002501
50×50	5000	0.001507
70×70	7000	0.001079
100×100	10000	0.000756
200×200	20000	0.000379
E.C.O = 0.99		

Table 2: Error in norm L^∞.

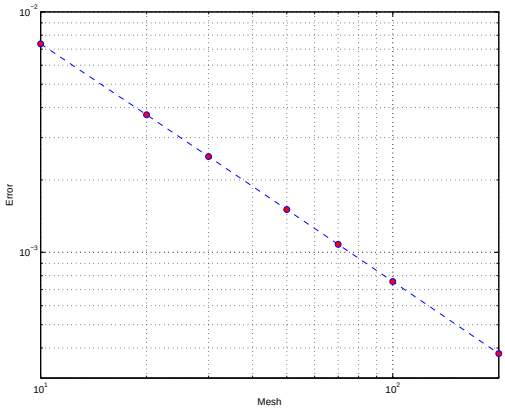

Figure 10: Mesh convergence in norm L^∞.

- **Adaptation of the first order scheme at the "outgoing boundaries"**

In dimension $d = 2$, the equations of the rays are given by

$$\begin{cases} \dot{x}(s, y_0) &= u_0(x,y) + c_0(x,y)\dfrac{\partial_x \phi(t,x,y)}{|\nabla \phi(t,x,y)|} \\ \dot{y}(s, y_0) &= v_0(x,y) + c_0(x,y)\dfrac{\partial_y \phi(t,x,y)}{|\nabla \phi(t,x,y)|} \end{cases}.$$

The rays are outgoing for the computational domain iff: $(\dot{x}, \dot{y}).\boldsymbol{n}(x,y) > 0$, where $\boldsymbol{n}(x,y)$ is the outward normal unit vector at the boundary at the point (x,y).

Remark 4.5. *We suppose here that the rays are transversal to $\partial\Omega$. We exclude the* ***glancing*** *case, i.e. $\boldsymbol{v}_g.\boldsymbol{n}_{|\partial\Omega} \neq 0$.*

By coupling the conditions above with the boundary conditions on the velocity field of the mean flow: $\boldsymbol{u}_0.\boldsymbol{n}_{|\partial\Omega} = 0$, the scheme at the rigid boundary is written:

➢ **On the edge** y_{min}**:** $i \in [\![0, I]\!]$

$$\phi_{i,0}^{n+1} = \phi_{i,0}^{n} - \triangle t \left(u_0^+ u_l - u_0^- u_r + c_0 \sqrt{\max^2(u_l^+, u_r^-) + v_r^{-2}} \right)_{|(x_i, y_0)} .$$

➢ **On the edge** y_{max}**:** $i \in [\![0, I]\!]$

$$\phi_{i,J}^{n+1} = \phi_{i,J}^{n} - \triangle t \left(u_0^+ u_l - u_0^- u_r + c_0 \sqrt{\max^2(u_l^+, u_r^-) + v_l^{+2}} \right)_{|(x_i, y_J)} .$$

➢ **On the edge** x_{max}**:** $j \in [\![0, J]\!]$

On the edge $\{x = x_{max}\}$, we require that the average flow is outgoing, *i.e.* $\boldsymbol{u}_0.\boldsymbol{n}_{|x_{max}} > 0$. So if the ray field is transversal to $\{x = x_{max}\}$, the scheme is written:

$$\phi_{I,j}^{n+1} = \phi_{I,j}^{n} - \triangle t \left(u_0^+ u_l + v_0^+ v_l - v_0^- v_r + c_0 \sqrt{u_l^{-2} + \max^2(v_l^+, v_r^-)} \right)_{|(x_I, y_j)} .$$

We propose to test the adaptation of the interior scheme at the boundary on the case of shear flow in a homogeneous medium (35). The velocity of the mean field is in the form $u_0(y) = 0.1 + 0.3y$, the incidence angle is $\alpha = \pi/4$, and the C.F.L. being 0.5.

$\boldsymbol{u_0(y) = 0.1 + 0.3y, \alpha = \pi/4}$		
Mesh	Iterations	Error L^∞
10×10	1000	0.007462
20×20	2000	0.003761
30×30	3000	0.002515
50×50	5000	0.001512
70×70	7000	0.001081
100×100	10000	0.000758
200×200	20000	0.000379
E.C.O = 0.99		

Table 3: Error in L^∞ norm.

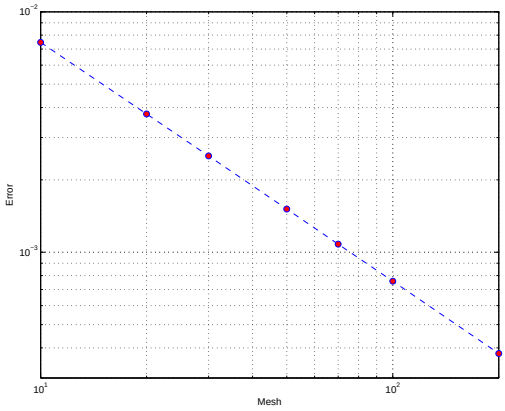

Figure 11: Mesh convergence in norm L^∞.

In order to illustrate the convergence of the approach presented in this paragraph, the error in the L^∞ norm, between the numerical phase and the analytic one (35), was calculated. These results are presented in the table above, and the figure is the logarithmic representation of this table.

In conclusion, the numerical experiments show that both approaches (extrapolation and adaptation) give the same order of error with a convergence of order one. We will see later that the situation is not the same for the second order scheme.

4.5 Numerical study of stability by mesh refinement

We consider that the incident wave is a plane wave given on the edge $\{x = 0\}$ with an incidence angle $\alpha = \pi/7$, and outgoing conditions are imposed on the other boundaries of the computational domain. The mean flow is a Poiseuille type flow: $u_0(y) = 0.1 + 0.4y^2$. We test here the stability of the scheme by mesh refinement. Given a time t_0, we thus compare the values of the phase computed on two grids with 50×50 and 200×200 elements. The number of iterations is chosen to match the same final time t_0 of simulation.

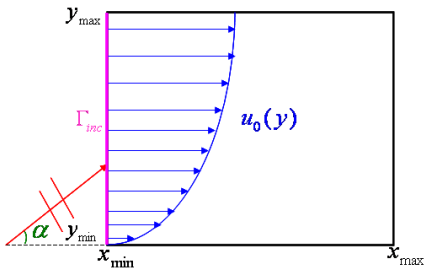

Figure 12: Poiseuille type flow.

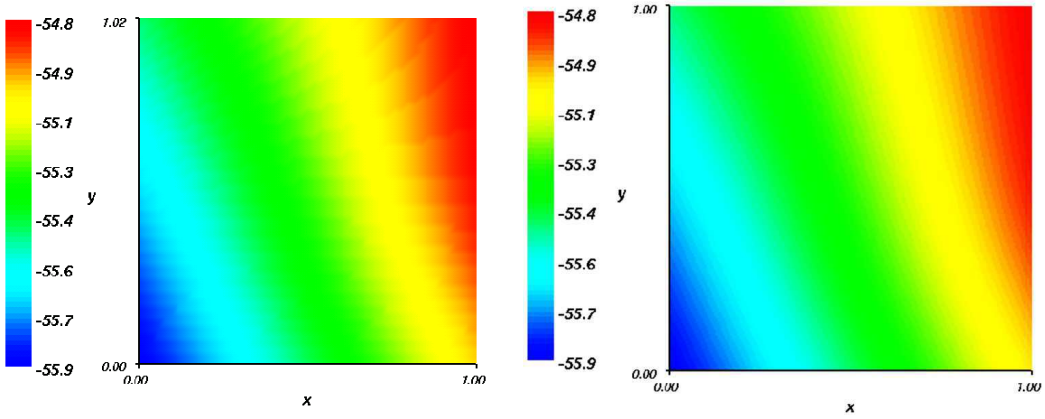

Figure 13: Left: 50×50 mesh,5000 iterations, Right: 200×200 mesh, 50000 iterations.

4.6 Second order Eulerian numerical scheme

It is shown (Harten *et al.* [17]) that monotone schemes in conservative form are necessarily of order one. In order to increase the precision of the numerical scheme (32) and preserve the monotony, we perform a construction by blocks of the numerical Hamiltonian $\hat{H}$, in which the first order approximations of the gradient of the phase are replaced by approximations of type Essentially Non Oscillatory (ENO) of high-order. To solve the whole problem, a second order accuracy for the eikonal equation is necessary to have an approximation of order one on the gradient of the phase in the transport equations (29) and (30).

4.6.1 Description of the second order scheme

The ENO schemes have been adapted to Hamilton-Jacobi equations by Shu and Osher in 1991. Here, we give the ENO construction of order two in space, and we refer to [34] for details and extension to higher orders. For an explicit scheme of second order in time, it is natural to calculate the phase ϕ at time offset by half a time step by the Heun scheme (second order Runge-Kutta scheme).

The second order numerical scheme is written with the same numerical Hamiltonian (33) and the approximation for the gradient of the phase is performed at second order accuracy:

$$\phi_{i,j}^{n+1} = \phi_{i,j}^{n} - \Delta t \hat{H}^{\pm}(t_n, x_i, y_j, u_l, u_r, v_l, v_r), \tag{38}$$

where:

$$\bullet u_l = D^{-x}\phi_{i,j}^{n} + \frac{\Delta x}{2}\text{minmod}(D^{-x}D^{-x}\phi_{i,j}^{n}, D^{+x}D^{-x}\phi_{i,j}^{n}),$$

$$\bullet u_r = D^{+x}\phi_{i,j}^{n} - \frac{\Delta x}{2}\text{minmod}(D^{+x}D^{+x}\phi_{i,j}^{n}, D^{+x}D^{-x}\phi_{i,j}^{n}),$$

$$\bullet v_l = D^{-y}\phi_{i,j}^{n} + \frac{\Delta y}{2}\text{minmod}(D^{-y}D^{-y}\phi_{i,j}^{n}, D^{+y}D^{-y}\phi_{i,j}^{n}),$$

$$\bullet v_r = D^{+y}\phi_{i,j}^{n} - \frac{\Delta y}{2}\text{minmod}(D^{+y}D^{+y}\phi_{i,j}^{n}, D^{+y}D^{-y}\phi_{i,j}^{n}),$$

with D^{-x} and D^{+x} denote the finite difference operator of first order, with respect to the variable x, upwinded to the left and right (and similarly for y), and the slope limiter is defined by

$$\text{minmod}(u,v) = \frac{\text{sgn}(u)+\text{sgn}(v)}{2}\min(|u|,|v|),$$

where sgn is the sign function. For better readability, the numerical scheme (38) is rewritten in the following way:

$$\phi_{i,j}^{n+1} = \hat{G}(\phi_{i\pm2,j\pm2}^{n}, \phi_{i\pm1,j\pm1}^{n}, \phi_{i,j}^{n}).$$

The space scheme has been performed with a second order accuracy. In order to respect the same order on the temporal accuracy, the Heun scheme is employed:

$$\phi_{i,j}^{n+1} = \frac{\phi_{i,j}^{n} + \tilde{\tilde{\phi}}_{i,j}}{2},$$

where $\tilde{\tilde{\phi}}_{i,j} = \hat{G}(\tilde{\phi}_{i\pm2,j\pm2}, \tilde{\phi}_{i\pm1,j\pm1}, \tilde{\phi}_{i,j})$ and $\tilde{\phi}_{i,j} = \hat{G}(\phi_{i\pm2,j\pm2}^{n}, \phi_{i\pm1,j\pm1}^{n}, \phi_{i,j}^{n})$.

4.6.2 Numerical test cases of second order scheme

➢ Test case I: Shear flow in a homogeneous medium

Consider first the mean field profile developed in the previous section (35) with $u_0(y) = 0.2y + 0.1$. It always uses the trace of the analytical phase on the edge $\{x = 0\}$ as incident condition. The numerical phase on the other edges is calculated by **an adaptation to order one of the interior scheme** (outgoing conditions). We have compared the analytical solution (35) to the numerical approximation for different meshes. The table below shows the mesh convergence in L^∞ norm, and the figure is a logarithmic representation of the table. The results show convergence with order two.

$u_0(y) = 0.1 + 0.2y, \alpha = \pi/4$		
Mesh	Iterations	Error L^∞
10×10	1000	1.0×10^{-4}
20×20	2000	$2{,}5\times10^{-5}$
40×40	4000	$6{,}0\times10^{-6}$
80×80	8000	$1{,}5\times10^{-6}$
160×160	16000	$3{,}8\times10^{-7}$
200×200	20000	$2{,}5\times10^{-7}$
E.C.O = 2.00		

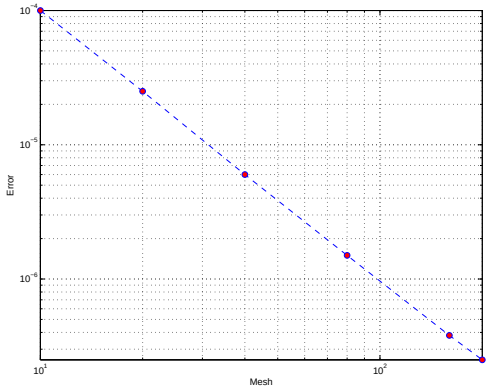

Table 4: Error in norm L^∞. Figure 14: Mesh convergence in norm L^∞.

➢ **Test case II: Analytical solution with outgoing conditions**

We consider the domain $[0,1]\times[0,1]$, filled with a static inhomogeneous medium, characterized by the speed of sound as follows:

$$c_0(x,y)=\frac{ax+\frac{b}{2}\left(y-\frac{1}{2}\right)^2+c}{\sqrt{a^2+b^2(y-\frac{1}{2})^2}},$$

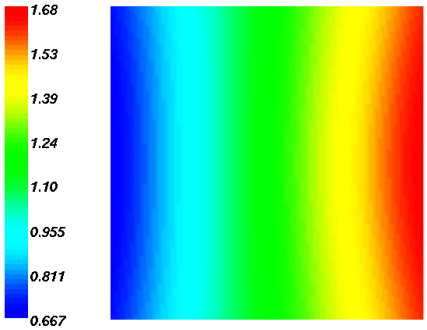

Figure 15: Sound speed profile.

where a, b, and c are reals parameters.

One can verify that a solution to the eikonal equation $\partial_t\phi+c_0(x,y)|\nabla\phi|=0$, is given by

$$\phi(t,x,y)=-t+\ln\left(ax+\frac{b}{2}\left(y-\frac{1}{2}\right)^2+c\right). \tag{39}$$

Remark 4.6. *If the parameters a and b are strictly positive, this solution is outgoing on the edges $\{x_{max}=1\}$, $\{y_{min}=0\}$, and $\{y_{max}=1\}$.*

The numerical experiment is performed with the following parameters: $a=1.5$, $b=1.5$ and $c=1$. We take the C.F.L. condition equal to 0.5. The numerical scheme was applied with three approaches for treating the outgoing conditions on $\partial\Omega\setminus\Gamma_{inc}$. Besides the two approaches explored previously (see subsection 4.4), we investigate a second order adaptation where we implement a scheme of order two until to the "outgoing boundaries".

In what follows, we verify the order of the scheme by mesh refinement for the three approaches. The tables below represent the error in the L^∞ norm as a function of the number of cells at $t=1.2$. We can see that for a ratio of two between the number of cells in each direction, the error is divided by four to a few percent which confirms the second order accuracy of the scheme. This fact is verified by the figures who are the logarithmic illustrations of the tables. Indeed, we note that all the errors behave as a straight of slope ~ -2 as a function of mesh refinement.

- **Extrapolation of the phase on the outgoing boundaries**

Mesh	Iterations	Error L^∞
15×15	1000	$1{,}1\times10^{-2}$
30×30	2000	$2{,}6\times10^{-3}$
60×60	4000	$6{,}4\times10^{-4}$
90×90	6000	$2{,}8\times10^{-4}$
120×120	8000	$1{,}6\times10^{-4}$
150×150	10000	9.8×10^{-5}
E.C.O = 2.04		

Table 5: Error in norm L^∞.

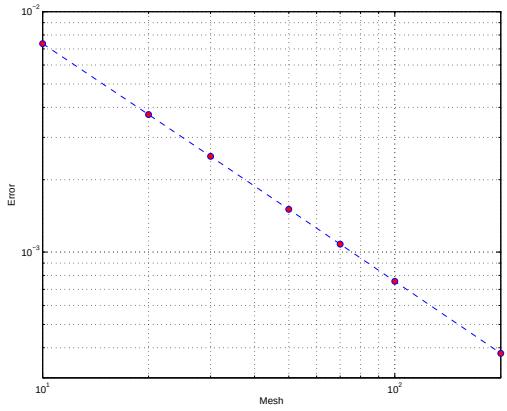

Figure 16: Mesh convergence in norm L^∞.

- **Adapting the scheme to the first order on the outgoing boundaries**

Mesh	Iterations	Error L^∞
15×15	1000	$4{,}2\times10^{-3}$
30×30	2000	$1{,}3\times10^{-3}$
60×60	4000	$3{,}9\times10^{-4}$
90×90	6000	$1{,}8\times10^{-4}$
120×120	8000	$1{,}1\times10^{-4}$
150×150	10000	$7{,}2\times10^{-5}$
E.C.O = 1.77		

Table 6: Error in norm L^∞.

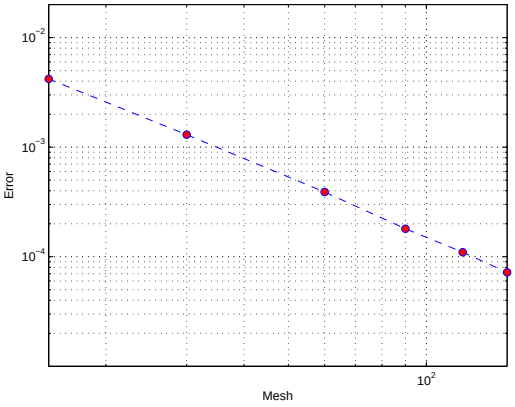

Figure 17: Mesh convergence in norm L^∞.

- **Adapting the scheme to the second order on the outgoing boundaries**

Mesh	Iterations	Error L^∞
15×15	1000	$1{,}2\times10^{-3}$
30×30	2000	$3{,}2\times10^{-4}$
60×60	4000	$8{,}5\times10^{-5}$
90×90	6000	$3{,}8\times10^{-5}$
120×120	8000	$2{,}2\times10^{-5}$
150×150	10000	$1{,}4\times10^{-5}$
E.C.O = 1.93		

Table 7: Error in norm L^∞.

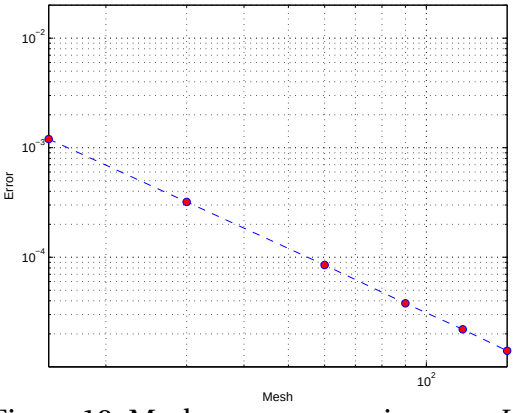

Figure 18: Mesh convergence in norm L^∞.

The results are in good agreement, for the three approaches, with the analytic solution. However, in order to make a comparison between them, the convergence rates for each approach, using other meshes, are presented in the figure 19. One can observe from this figure that, in agreement with the previous results, the order of the scheme is preserved for the three approaches. Note also that the extrapolation approach is less accurate than both other ones. In conclusion, we can say that the adaptation to order one, of the interior scheme at the "outgoing boundaries", gives a good balance between the order of accuracy and the easiness of numerical implementation. Also note that, for the second order adaptation, not using slope limiter at the vicinity of the edge can generate oscillations.

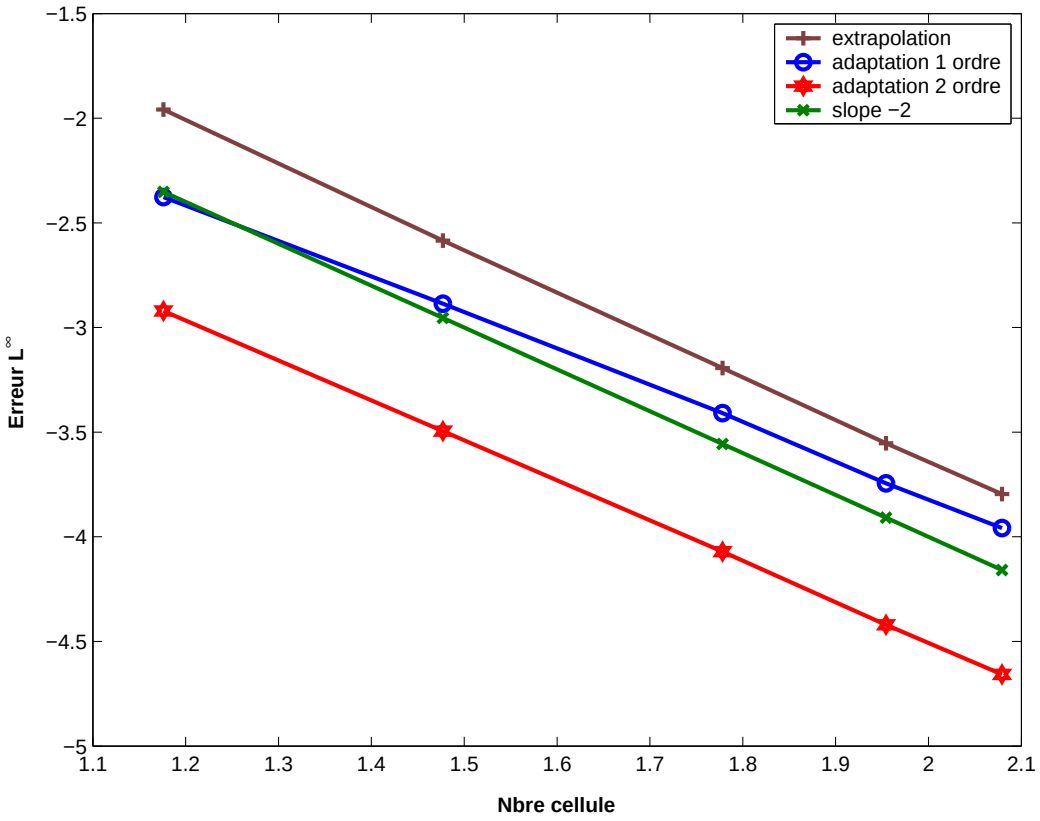

Figure 19: Comparison of convergence rates.

5 Computation of the stretching matrix

A new and important feature of this paper is to compute the geometrical optics approximation of the acoustic perturbation using the Eulerian approach. For this, the geometric spreading is calculated on a fixed grid by solving the transport equation (29) with no integration of the Hamiltonian vector field. We recall that, according to the subsection 3.2, the geometrical spreading G is given by

$$G = \begin{vmatrix} 1 & & \\ & \Theta & \\ \boldsymbol{v}_g & & \end{vmatrix},$$

where Θ is the first matrix in the stretching matrix $U = \begin{pmatrix} \Theta \\ \Lambda \end{pmatrix}$ defined in (28) and solution of the equation (29).

Assume the numerical calculation of the phase ϕ has already been done, the approximation of the group velocity $\boldsymbol{v}_g$ is directly given by a discretized gradient of ϕ.

In what follows, we present a numerical scheme of order one in two dimensions of space that allows all calculations of the high frequency approximation of the acoustic quantities on an Eulerian grid by solving the transport equation (29).

5.1 Construction of the numerical scheme

• Approximation of the gradient of the phase

We write an explicit first order scheme for the transport equation (29), *i.e.*

$$\partial_t U + H_\xi(\nabla\phi)\partial_x U + H_\zeta(\nabla\phi)\partial_y U = \mathscr{M}(\nabla\phi)U,$$

the advection field of the equation (29) is the group velocity while its source term involves the second derivatives of the Hamiltonian H.

The advection field and source term of the equation (29) are functions of the gradient of the phase ϕ. By eliminating the assumption of a privileged direction of propagation, it seemed that the most natural choice was to make a centered average gradient of the phase at the centers of the cells:

$$(\partial_x \phi)^n_{(i+1/2,j+1/2)} = \frac{D^{-x}\phi^n_{i+1,j+1} + D^{-x}\phi^n_{i+1,j}}{2},$$
$$(\partial_y \phi)^n_{(i+1/2,j+1/2)} = \frac{D^{-y}\phi^n_{i+1,j+1} + D^{-y}\phi^n_{i,j+1}}{2}.$$

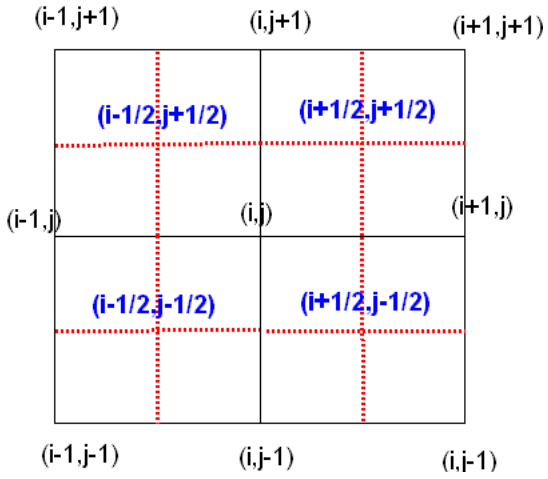

Figure 20: Staggered mesh for the computation of the geometrical spreading.

The equations (29) and (30) are approximated in a staggered mesh. In this mesh, **the geometrical spreading and the function $\mathscr{C}$, and thereafter the acoustic quantities are all calculated at the centers of the cells**. Recall that the phase ϕ was calculated at the grid points. Its value at the cell centers is approximated by the averaging. **Note that contrarily to the ray tracing method, one does not need to calculate the bicharacteristics to obtain the geometrical optic approximation of the acoustic perturbation**.

• Construction of the numerical scheme

The equation (29) involves two processes, namely advection and diffusion. Conventionally, we split the advection-diffusion equation into an advection equation and an ordinary differential equation (ODE), each of which will be solved separately (an advection step followed by a diffusion step). For the time integration of the diffusion part (step 1), we compute explicitly the exponential matrix of $\mathscr{M}$. On the other hand, the advection part (step 2) is discretized by an upwind scheme.

Assuming that the discrete approximation U^n, of the solution of (29) at time $t_n = n\triangle t$, has been computed, the next approximation U^{n+1} is constructed as following:

Step1:

$$\partial_t U^* = \mathscr{M}(\nabla\phi)U^* \text{ on } [0,\triangle t], \text{ with } U^*(0) = U^n$$

Step2:

$$\partial_t U^{**} + H_\xi(\nabla\phi)\partial_x U^{**} + H_\zeta(\nabla\phi)\partial_y U^{**} = 0 \text{ on } [0,\triangle t], \text{ with } U^{**}(0) = U^*(\triangle t)$$

and setting

$$U^{n+1} = U^{**}(\triangle t).$$

Each of these two steps above are tested and validated before proceeding to the test case on the full equation (29).

5.2 Scheme for the advection part

• Description of the scheme

The approximation of the advection equation is chosen simply by the upwind scheme in the direction of the group velocity:

$$\frac{U_{i,j}^{n+1} - U_{i,j}^n}{\triangle t} + s_1 H_\xi(\nabla\phi^n_{i+1/2,j+1/2})\frac{U_{i,j}^n - U_{i-s1,j}^n}{\triangle x} + s_2 H_\zeta(\nabla\phi^n_{i+1/2,j+1/2})\frac{U_{i,j}^n - U_{i,j-s_2}^n}{\triangle y} = 0, \quad (40)$$

where $s_1 = \text{sgn}(H_\xi(\nabla\phi^n_{i+1/2,j+1/2}))$ and $s_2 = \text{sgn}(H_\zeta(\nabla\phi^n_{i+1/2,j+1/2}))$, with sgn is the sign function.

• Test case for the advection step

The purpose of this numerical test case is to show that a more precise computation of the gradient of the phase does not improve the precision on U.

We consider a static fluid medium in which the speed of sound is affine:

$$c_0(x,y) = ax + by + c.$$

By integration of the field of bicharacteristics and the fact that the phase is preserved along the Hamiltonian flow, we compute an analytical solution of the

eikonal equation in the acoustic mode +, given by:

$$\phi(t,x,y) = -t + \frac{1}{\sqrt{a^2+b^2}} \ln(ax+by+c). \tag{41}$$

By integrating the transport equation on $\boldsymbol{U}$ without the source term, *i.e.*

$$\partial_t \boldsymbol{U} + H_\xi(\boldsymbol{\nabla}\phi)\partial_x \boldsymbol{U} + H_\zeta(\nabla\phi)\partial_y \boldsymbol{U} = 0,$$

along the ray field whose the incident phase is given by the trace of (41) on the surface $\{x=0\}$, we obtain an analytic expression for $\boldsymbol{U}$:

$$\boldsymbol{U}(t,x,y) = \begin{pmatrix} \dfrac{-ab}{\sqrt{a^2+b^2}} \dfrac{e^{2t\sqrt{a^2+b^2}}}{(ax+by+c)^2} \\ \dfrac{-b^2}{\sqrt{a^2+b^2}} \dfrac{e^{2t\sqrt{a^2+b^2}}}{(ax+by+c)^2} \\ \dfrac{-ab}{\sqrt{a^2+b^2}} e^{-2t\sqrt{a^2+b^2}} (ax+by+c)^2 \\ \dfrac{-b^2}{\sqrt{a^2+b^2}} e^{-2t\sqrt{a^2+b^2}} (ax+by+c)^2 \end{pmatrix}.$$

The table below represents the difference between the numerical approximation and the analytical solution in the L^∞ norm. It can be seen that the order 1 of the scheme is validated.

Mesh	Iterations	Error $U[1]$	Error $U[2]$	Error $U[3]$	Error $U[4]$
50×50	1000	2.5×10^{-3}	1.3×10^{-3}	1.0×10^{-5}	5.3×10^{-6}
100×100	2000	1.3×10^{-3}	6.5×10^{-4}	5.2×10^{-6}	2.6×10^{-6}
200×200	4000	6.7×10^{-4}	3.3×10^{-4}	2.6×10^{-6}	1.3×10^{-6}
400×400	8000	3.4×10^{-4}	1.7×10^{-4}	1.3×10^{-6}	6.5×10^{-7}

Table 8: Mesh convergence in norm L^∞ at fixed time.

We have compared the results of the table aforementioned with those obtained with an analytical gradient of the phase ϕ. For this, we deduce the gradient of the phase explicitly from the analytical expression (41), and we have injected it into the numerical scheme (40). We have observed that both approaches (analytical and numerical gradient) give the same order of magnitude of the error on U. This can be explained by the fact that the error of the numerical scheme is dominating compared to the error due to the calculation of the advection field, which somewhat hides the improvement of computing the

gradient of the phase. Therefore, even by increasing the order of the scheme for solving the eikonal equation, this is not going to improve the accuracy on the computation of $\boldsymbol{U}$.

5.3 Scheme for the diffusion part

The matrix $\mathscr{M}$ is given explicitly by the second derivatives of the Hamiltonian H. Then, the ordinary differential equation

$$\partial_t U = \mathscr{M}(\boldsymbol{\nabla}\phi)U \tag{42}$$

can be solved by computing the exponential matrix *of* $\mathscr{M}$ at each time step and at each grid point. In the following we give an explicit expression of the exponential matrix of $\mathscr{M}$ using its structure. However, this does not give us the exact solution of (42) because $\mathscr{M}$ depends on the gradient of the phase ϕ.

• Computation of the exponential matrix

The matrix $\mathscr{M}$ is of the form

$$\mathscr{M} = \begin{pmatrix} A & B \\ C & -A^t \end{pmatrix},$$

where $C = C^t$ and $B = B^t$. It is precisely in **the Lie algebra of the Hamiltonian matrix**. It follows that:

Lemma 5.1. *If λ is an eigenvalue of the matrix $\mathscr{M}$, then $-\lambda$, $\bar{\lambda}$, and $-\bar{\lambda}$ are also eigenvalues of $\mathscr{M}$ with the same multiplicity.*

One deduces then that the characteristic polynomial $p_{\mathscr{M}}$ of the matrix $\mathscr{M}$ is an even polynomial, more precisely it is written as

$$p_{\mathscr{M}}(\lambda) = \lambda^4 + \alpha\lambda^2 + \beta, \tag{43}$$

where

$$\begin{cases} \alpha &= 2\left(H_{x\xi}H_{y\zeta} - H_{y\xi}H_{x\zeta}\right) - (H_{y\zeta} + H_{x\xi})^2 + \dfrac{c_0(\xi^2 H_{yy} + \zeta^2 H_{xx} - 2\xi\zeta H_{xy})}{(\xi^2+\zeta^2)^{3/2}} \\ \\ \beta &= \left(H_{x\xi}H_{y\zeta} - H_{y\xi}H_{x\zeta}\right)^2 + \dfrac{c_0\left(2H_xH_yH_{xy} - H_{xx}H_y^2 - H_{yy}H_x^2\right)}{(\xi^2+\zeta^2)^{3/2}}. \end{cases}$$

Two different cases arise:

1. if the polynomial $p_{\mathscr{M}}$ has simple roots $(\lambda_i)_{1\le i\le 4}$, the exponential matrix of $\mathscr{M}$ is given nicely by $e^{\mathscr{M}} = \mathscr{P}\, e^{\mathscr{D}} \mathscr{P}^{-1}$, where $\mathscr{D} = \mathrm{diag}(\lambda_1,\lambda_2,\lambda_3,\lambda_4)$ with $\mathscr{P}$ being the change of basis matrix.

2. if there is a double root of the polynomial $p_{\mathscr{M}}$, by the Cayley-Hamilton theorem, there exist constants $a_k(\alpha,\beta)$ such that we have:

$$\mathscr{M}^{2k} = a_k(\alpha,\beta)\mathscr{M}^2 + \mathscr{N}, \quad \text{where } \mathscr{N}^2 = 0. \tag{44}$$

Therefore, since $\exp(\mathscr{M}) = \sum_{k=0}^{+\infty} \frac{\mathscr{M}^k}{k!}$, the exponential is calculated using recurrence formula (44) following the table (10).

• Test case for the diffusion part

We interest ourselves in the basic shear flow of the form $u_0(y) = M_0 + M_0' y$, in a homogeneous medium ($c_0 = 1$). By the explicit expressions (37) and (35), we show that the matrix $\mathscr{M}$ is

$$\mathscr{M}(\nabla\phi) = \begin{pmatrix} 0 & M_0' & \frac{\eta_2^2}{(\eta_2^2+\eta_1^2)^{\frac{3}{2}}} & \frac{\eta_2\eta_1}{(\eta_2^2+\eta_1^2)^{\frac{3}{2}}} \\ 0 & 0 & \frac{\eta_2\eta_1}{(\eta_2^2+\eta_1^2)^{\frac{3}{2}}} & \frac{\eta_1^2}{(\eta_2^2+\eta_1^2)^{\frac{3}{2}}} \\ 0 & 0 & 0 & 0 \\ 0 & 0 & -M_0' & 0 \end{pmatrix},$$

where $\eta_1 = \cos\alpha$ and $\eta_2 = \sin\alpha - M_0' t\cos\alpha$.

One can verify that $\boldsymbol{U}(t,x,y) = \left(C_2 M_0' t + C_1, C_2, -\eta_1, \eta_2\right)^t$ is a solution of (42), where C_1 and C_2 are constants.

To check the order of the scheme in time, we set the mesh 50×50 and a time T, and we refine the time step to arrive at time T:

Δt	Nbre Iter	ErrL^∞ U[1]	ErrL^∞ U[2]	ErrL^∞ U[3]	ErrL^∞ U[4]
6×10^{-3}	1000	6.31×10^{-4}	3.1×10^{-3}	0.	5.49×10^{-15}
3×10^{-3}	2000	3.17×10^{-4}	1.59×10^{-3}	0.	2.51×10^{-14}
1.5×10^{-3}	4000	1.59×10^{-4}	7.98×10^{-4}	0.	2.90×10^{-14}
7.5×10^{-4}	8000	7.9×10^{-5}	3.99×10^{-4}	0.	6.41×10^{-14}

Table 9: Convergence in time.

We observe in the table above that the error is approximatively reduced by a factor of 2 which confirms the order 1 of the scheme.

Parameters	Exponential matrix of $\mathscr{M}$
$\beta=0,\ \alpha=0$	$e^{t\mathscr{M}}=I_4+t\mathscr{M}+\frac{t^2}{2}\mathscr{M}^2+\frac{t^3}{6}\mathscr{M}^3$
$\beta=0,\ \alpha<0$	$\lambda=\sqrt{\lvert\alpha\rvert}\,,\ e^{t\mathscr{M}}=I_4+t\mathscr{M}+\frac{\cosh(\lambda t)-1}{\lambda^2}\mathscr{M}^2+\frac{\sinh(\lambda t)-\lambda t}{\lambda^3}\mathscr{M}^3.$
$\beta=0,\ \alpha>0$	$\lambda=\sqrt{\alpha}\,,\ e^{t\mathscr{M}}=I_4+t\mathscr{M}-\frac{\cos(\lambda t)-1}{\lambda^2}\mathscr{M}^2-\frac{\sin(\lambda t)-\lambda t}{\lambda^3}\mathscr{M}^3.$
$\beta=\frac{\alpha^2}{4},\ \alpha<0$	$\lambda=\sqrt{\frac{\lvert\alpha\rvert}{2}}\,,\ e^{t\mathscr{M}}=\frac{2\cosh(\lambda t)-\lambda t\sinh(\lambda t)}{2}I_4+\frac{3\sinh(\lambda t)-\lambda t\cosh(\lambda t)}{2\lambda}\mathscr{M}+\frac{t\sinh(\lambda t)}{2\lambda}\mathscr{M}^2+\frac{\lambda t\cosh(\lambda t)-\sinh(\lambda t)}{2\lambda^3}\mathscr{M}^3.$
$\beta=\frac{\alpha^2}{4},\ \alpha>0$	$\lambda=\sqrt{\frac{\alpha}{2}}\,,\ e^{t\mathscr{M}}=\frac{2\cos(\lambda t)+\lambda t\sin(\lambda t)}{2}I_4+\frac{3\sin(\lambda t)-\lambda t\cos(\lambda t)}{2\lambda}\mathscr{M}+\frac{t\sin(\lambda t)}{2\lambda}\mathscr{M}^2+\frac{\sin(\lambda t)-\lambda t\cos(\lambda t)}{2\lambda^3}\mathscr{M}^3\,.$
$0<\beta<\frac{\alpha^2}{4},\ \alpha<0$	$\lambda=\left(\frac{-\alpha+\sqrt{\alpha^2-4\beta}}{2}\right)^{1/2},\ \mu=\left(\frac{-\alpha-\sqrt{\alpha^2-4\beta}}{2}\right)^{1/2},\ e^{t\mathscr{M}}=\mathscr{P}^{-1}\begin{pmatrix}e^{t\lambda}&0&0&0\\0&e^{-t\lambda}&0&0\\0&0&e^{t\mu}&0\\0&0&0&e^{-t\mu}\end{pmatrix}\mathscr{P}$
$0<\beta<\frac{\alpha^2}{4},\ \alpha>0$	$\mu=\left(\frac{\alpha+\sqrt{\alpha^2-4\beta}}{2}\right)^{1/2},\ \nu=\frac{\sqrt{2\beta}}{\left(\alpha+\sqrt{\alpha^2-4\beta}\right)^{1/2}},\ e^{t\mathscr{M}}=\mathscr{P}^{-1}\begin{pmatrix}\cos(\mu t)&\sin(\mu t)&0&0\\-\sin(\mu t)&\cos(\mu t)&0&0\\0&0&\cos(\nu t)&\sin(\nu t)\\0&0&-\sin(\nu t)&\cos(\nu t)\end{pmatrix}\mathscr{P}.$
$\frac{\alpha^2}{4}<\beta$	$\mu=\frac{\sqrt{2\sqrt{\beta}-\alpha}}{2},\ \nu=\frac{\sqrt{2\sqrt{\beta}+\alpha}}{2},\ e^{t\mathscr{M}}=\mathscr{P}^{-1}\begin{pmatrix}e^{t\mu}\cos(\nu t)&e^{t\mu}\sin(\nu t)&0&0\\e^{t\mu}\sin(-\nu t)&e^{t\mu}\cos(\nu t)&0&0\\0&0&e^{-t\mu}\cos(\nu t)&e^{-t\mu}\sin(\nu t)\\0&0&e^{-t\mu}\sin(-\nu t)&e^{-t\mu}\cos(\nu t)\end{pmatrix}\mathscr{P}.$
$\beta<0$	$\mu=\left(\frac{-\alpha+\sqrt{\alpha^2-4\beta}}{2}\right)^{1/2},\nu=\left\lvert\frac{-\alpha-\sqrt{\alpha^2-4\beta}}{2}\right\rvert^{1/2},e^{t\mathscr{M}}=\mathscr{P}^{-1}\begin{pmatrix}e^{t\mu}&0&0&0\\0&e^{-t\mu}&0&0\\0&0&\cos(t\nu)&\sin(t\nu)\\0&0&-\sin(t\nu)&\cos(t\nu)\end{pmatrix}\mathscr{P}.$

Table 10: The exponential matrix of $\mathscr{M}$ according to the parameters values.

5.4 Test case of the splitting scheme

In this subsection, we test the full scheme (advection and diffusion) on a numerical test case in a inhomogeneous medium at rest. We examine the mesh convergence, and we also give the error in the L^∞ norm on the constant along ray field and on the acoustic pressure.

• Analytical solution

In this test case, we derive an explicit expression for the zero order approximation of the acoustic quantities. For this, we study the acoustic propagation in a inhomogeneous medium at rest in which the speed of sound is:

$$c_0(x,y) = \frac{(x+a)(y+b)}{\sqrt{(x+a)^2+(y+b)^2}}$$

A solution of the eikonal equation associated with the acoustic mode +

$$\partial_t \phi + c_0(x,y)|\nabla\phi| = 0$$

is given by

$$\phi(t,x,y) = e^{-t}(x+a)(y+b). \tag{45}$$

Assume that the parameters $a, b \geq 1$, and we position ourselves in the subdomain $\{x \geq 0,\ y \geq 0\}$. We take as usual the incident phase as the trace of the analytical phase (45) on the incident surface $\Gamma_{inc} = \{(0,y_0);\ y_0 \in \mathbb{R}\}$.

When the phase is of the form $\phi(t,x,y) = \phi_1(t)\phi_2(x,y)$, Proposition C.1 (see Annexe C) assures us that the coordinates x and y are independent of the parameter t_0. As, on the other hand $\dot{t}(s,\boldsymbol{\alpha}) = 1$, it follows that the time variable can be considered as a curvilinear abscissa along the bicharacteristics.

Using the fact that the phase is conserved along the ray field, we deduce that

$$e^{-t}(x+a)(y+b) = a(y_0+b). \tag{46}$$

Since the ray field is solution of the system

$$\begin{cases} \dfrac{dx}{dt} = c_0(x,y)\dfrac{y+b}{\sqrt{(x+a)^2+(y+b)^2}} \\ \dfrac{dy}{dt} = c_0(x,y)\dfrac{x+a}{\sqrt{(x+a)^2+(y+b)^2}} \end{cases},$$

we show (by multiplying the first equation by $x+a$ and the second equation by $y+b$) that :

$$(x+a)^2-(y+b)^2=a^2-(y_0+b)^2. \tag{47}$$

By deriving the equations (46) and (47) with respect to the initial position of rays , we find:

$$\begin{cases} \dfrac{\partial x}{\partial y_0}=\dfrac{y+b}{a[(x+a)^2+(y+b)^2]}(a^2e^t-(x+a)^2e^{-t}) \\ \dfrac{\partial y}{\partial y_0}=\dfrac{x+a}{a[(x+a)^2+(y+b)^2]}(a^2e^t+(y+b)^2e^{-t}) \end{cases}.$$

Furthermore, we assume that the characteristic manifold and the Lagrangian submanifold, consisting of the union of bicharacteristics, coincide at initial time. By Proposition (2.9), they coincide at any time. This yields

$$\begin{cases} \xi(t,y_0)=\partial_x\phi(t,x(t,y_0),y(t,y_0))=e^{-t}(y(t,y_0)+b) \\ \zeta(t,y_0)=\partial_y\phi(t,x(t,y_0),y(t,y_0))=e^{-t}(x(t,y_0)+a) \end{cases},$$

thus we can write

$$\begin{cases} \partial_{y_0}\xi(t,y_0)=e^{-t}\partial_{y_0}y \\ \partial_{y_0}\zeta(t,y_0)=e^{-t}\partial_{y_0}x \end{cases}.$$

For the foregoing, we prove that a solution of the transport equation

$$\partial_t\boldsymbol{U}+H_\xi(\boldsymbol{\nabla}\phi)\partial_x\boldsymbol{U}+H_\zeta(\boldsymbol{\nabla}\phi)\partial_y\boldsymbol{U}=\mathscr{M}(\boldsymbol{\nabla}\phi)U,$$

associated with the phase (45), is given by

$$\boldsymbol{U}(t,x,y)=\frac{1}{a[(x+a)^2+(y+b)^2]}\begin{pmatrix} (y+b)[a^2e^t-(x+a)^2e^{-t}] \\ (x+a)[a^2e^t+(y+b)^2e^{-t}] \\ (x+a)[a^2+(y+b)^2e^{-2t}] \\ (y+b)[a^2-(x+a)^2e^{-2t}] \end{pmatrix}.$$

By Proposition C.1, the geometrical spreading is reduced to

$$G(t,x(t,y_0),y(t,y_0))=-\begin{vmatrix} \partial_t x(t,y_0) & \partial_{y_0}x(t,y_0) \\ \partial_t y(t,y_0) & \partial_{y_0}y(t,y_0) \end{vmatrix},$$

where

$$\begin{cases} \partial_t x(t,y_0)=H_\xi(x,y,\boldsymbol{\nabla}\phi(t,x,y)) \\ \partial_t y(t,y_0)=H_\zeta(x,y,\boldsymbol{\nabla}\phi(t,x,y)) \end{cases}.$$

We then find an expression for the Eulerian geometrical spreading

$$G(t,x,y)=\frac{(x+a)^2(y+b)^2e^{-t}}{a[(x+a)^2+(y+b)^2]}.$$

Using Proposition 3.4, we find

$$a_0(t,x,y)=\left(\frac{a\rho_0\left[(x+a)^2+(y+b)^2\right]^3}{(x+a)^3(y+b)^3}\right)^{\frac{1}{2}}.$$

where the function $\mathscr{C}$ of Proposition 3.4 is equal to 1.

In conclusion, the analytical expression, of the leading order term of the high frequency approximation, of the acoustic perturbation is expressed as:

$$\begin{pmatrix}\varrho\\ u\\ v\\ s\end{pmatrix}=a_0(t,x,y)\cos\left(ke^{-t}(x+a)(y+b)\right)\begin{pmatrix}1\\ \dfrac{(y+b)^2(x+a)}{\sqrt{(x+a)^2+(y+b)^2}}\\ \dfrac{(x+a)^2(y+b)}{(x+a)^2+(y+b)^2}\\ s_0\end{pmatrix}+O(k^{-1}),$$

and the main term of the asymptotic expansion of the acoustic pressure is calculated by

$$p(t,x,y)=c_0^2(x,y)a_0(t,x,y)\cos\left(ke^{-t}(x+a)(y+b)\right)+O(k^{-1}).$$

• Comparison with numerical solution

In the presentation below on a logarithmic scale, we note that all the errors, in L^∞ norm, behave as lines of slope ~ -1 depending on the mesh refinement. This confirms the order one of a scheme.

Mesh	Iter	$\boldsymbol{U}[1]$	$\boldsymbol{U}[2]$	$\boldsymbol{U}[3]$	$\boldsymbol{U}[4]$
50×50	1000	1.88×10^{-3}	1.25×10^{-3}	4.94×10^{-4}	$1.\times10^{-3}$
100×100	2000	1.01×10^{-3}	6.99×10^{-4}	2.8×10^{-4}	5.18×10^{-4}
200×200	4000	5.4×10^{-4}	3.86×10^{-4}	1.54×10^{-4}	2.67×10^{-4}
300×300	6000	3.6×10^{-4}	2.71×10^{-4}	1.07×10^{-4}	1.80×10^{-4}
400×400	8000	2.82×10^{-4}	2.11×10^{-4}	8.34×10^{-5}	1.37×10^{-4}
500×500	10000	2.3×10^{-4}	1.75×10^{-4}	6.96×10^{-5}	1.10×10^{-4}
E.C.O		0.91	0.85	0.85	0.95

Table 11: Mesh convergence in L^∞ norm for the components of U.

Mesh	Iter	$\mathscr{C}$	p
50×50	1000	1.42×10^{-2}	3.61×10^{-3}
100×100	2000	7.18×10^{-3}	1.72×10^{-3}
200×200	4000	3.6×10^{-3}	8.4×10^{-4}
300×300	6000	2.40×10^{-3}	5.54×10^{-4}
400×400	8000	1.8×10^{-3}	4.15×10^{-4}
500×500	10000	1.44×10^{-3}	3.26×10^{-4}
E.C.O		0.99	1.03

Table 12: Mesh convergence in L^∞ for $\mathscr{C}$ and p.

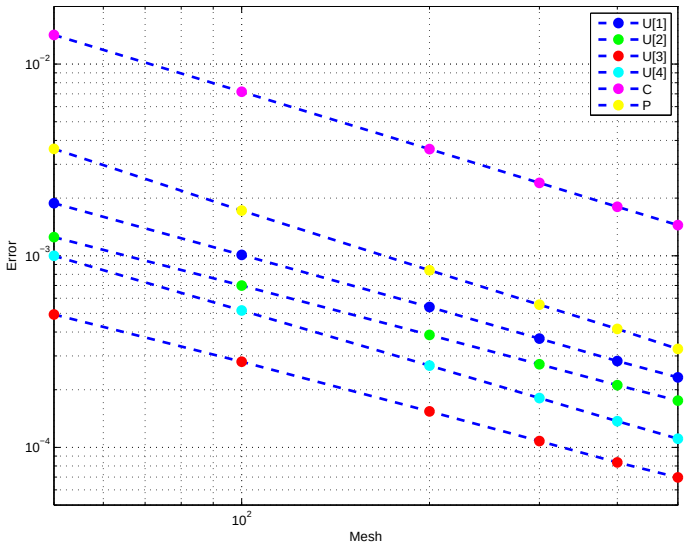

Figure 21: Mesh convergence in logarithmic scale.

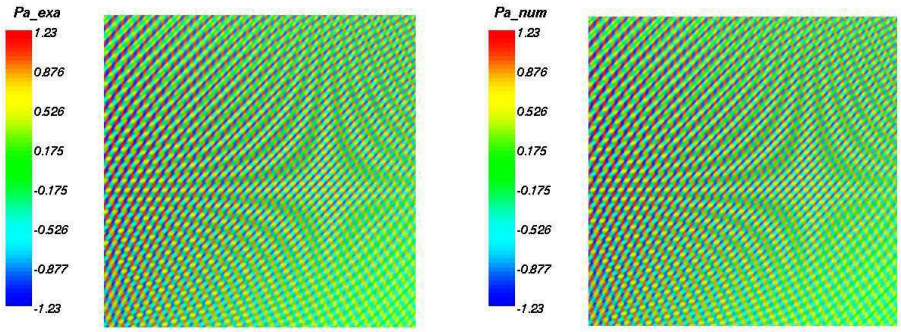

(a) Analytical acoustic pressure. (b) Numerical acoustic pressure.

Figure 22: Countour lines of the analytical and the numerical acoustic pressure.

6 Conclusion

We developed in this contribution a new approach for calculating the propagation of acoustic waves in the high frequency regime for any regular mean flow without restricting ourselves to constant or potential flows. Another original feature of this article, from a numerical point of view, is the choice of an Eulerian method for solving both the eikonal equation on the phase ϕ and the transport equation for the stretching matrix which is a more general tool from what is already used in [3]. The latter is the key quantity for computing the geometrical optics approximation of the acoustic perturbation. Hence, we obtain a generalization to a system of the results of Benamou *et al.* [2, 3] for a wave equation with non-constant sound velocity.

A crucial point in our study is the geometrical identification of a conserved quantity along the group velocity. We obtain that $\frac{a_0^2 c_0 J}{\rho_0 |\nabla \phi|}$ is conserved, where a_0 is the leading order term of the acoustic perturbation around the mean density ρ_0, c_0 is the sound velocity, J being the geometrical spreading. We compute J through the stretching matrix. Note that the existence of a conserved quantity is true for any hyperbolic operator, even a non conservative one, provided that we place ourselves on a leaf of the characteristic variety associated to a simple eigenvalue of the principal symbol of this operator [24]. In future works, one has to obtain a generic and geometric interpretation for this conserved quantity for any hyperbolic operator with such features.

From a numerical point of view, we develop a numerical scheme of order two for solving the eikonal equation. We achieved the implementation of this scheme despite max-min (min-max) difficulties in the numerical Hamiltonian of Godunov. Several test cases have been performed to find the more relevant numerical Hamiltonian which provides a good balance between the numerical diffusion and the monotony of the scheme. The scheme was validated, and the order of convergence has been checked by comparison with analytical explicit solutions.

Among the problems solved for the transport equation satisfied by the stretching matrix, the splitting between the advection and diffusion steps is crucial. The numerical scheme for solving this transport equation is implemented using the cell centers of the mesh used for solving the eikonal equation. This defines globally a fixed staggered mesh. This secondary grid has the advantage of not being linked to a preferred direction of propagation.

The numerical results obtained are extremely encouraging, especially when comparing with exact analytical solutions. The cost-effectiveness of the method should use cross validation with a direct solution method or with the ray tracing method.

The method developed in this contribution can be generalized in the neighborhood of a fold caustic. The analogous transport equation is presented in [32] and [24], and will be the center point of forthcoming publications which aim to calculate the amplitude of the solution in the presence of a fold caustic. Among the other problems that seem reachable using our method, we may mention the reflection of the acoustic wave by a boundary; preliminary results are available in [32].

Appendix A: Proof of Lemma 2.12

Lemma 2.12 *The eikonal equation on the phase $\phi^{\pm}$ is equivalent to the following one:*

$$\partial_t\left(\frac{1}{|\boldsymbol{\nabla}_x\phi^{\pm}|}\right)+\boldsymbol{v}_g^{\pm}.\boldsymbol{\nabla}_x\left(\frac{1}{|\boldsymbol{\nabla}_x\phi^{\pm}|}\right) = \frac{1}{|\boldsymbol{\nabla}_x\phi^{\pm}|^3}\boldsymbol{\nabla}_x\phi^{\pm}.\left(\boldsymbol{\nabla}_x\phi^{\pm}\overline{\overline{\otimes}}\overline{\overline{\nabla}}_x\boldsymbol{u}_0\right)\pm\frac{1}{|\boldsymbol{\nabla}_x\phi^{\pm}|^2}\boldsymbol{\nabla}_x\phi^{\pm}.\boldsymbol{\nabla}_x c_0.$$

Proof. First, we note that, for acoustic modes, the particle derivative of the phase $\phi^{\pm}$ along the mean flow velocity is non zero, which means it has no stationary points compared to the space variables (*i.e.* $\boldsymbol{\nabla}_{\boldsymbol{x}}\phi^{\pm}\neq 0$).

We assume that the phase $\phi^{\pm}$ is a regular function. By deriving the eikonal equation with respect to space variables, we find

$$\partial_t(\boldsymbol{\nabla}_x\phi^{\pm})+\overline{\overline{\nabla}}_x\boldsymbol{u}_0.\boldsymbol{\nabla}_x\phi^{\pm}+\overline{\overline{\nabla}}_x(\boldsymbol{\nabla}_x\phi^{\pm}).\boldsymbol{u}_0\pm|\boldsymbol{\nabla}_x\phi^{\pm}|\boldsymbol{\nabla}_x c_0\pm c_0\boldsymbol{\nabla}_x(|\boldsymbol{\nabla}_x\phi^{\pm}|)=0,$$

taking the scalar product of the above equation with the gradient of the phase $\phi^{\pm}$, we then obtain

$$\boldsymbol{\nabla}_x\phi^{\pm}.\partial_t(\boldsymbol{\nabla}_x\phi^{\pm})+\left(\overline{\overline{\nabla}}_x\boldsymbol{u}_0.\boldsymbol{\nabla}_x\phi^{\pm}\right).\boldsymbol{\nabla}_x\phi^{\pm}+\left(\overline{\overline{\nabla}}_x\left(\boldsymbol{\nabla}_x\phi^{\pm}\right).\boldsymbol{u}_0\right).\boldsymbol{\nabla}_x\phi^{\pm} \pm|\boldsymbol{\nabla}_x\phi^{\pm}|\boldsymbol{\nabla}_x\phi^{\pm}.\boldsymbol{\nabla}_x c_0\pm c_0\boldsymbol{\nabla}_x\phi^{\pm}.\boldsymbol{\nabla}_x\left(|\boldsymbol{\nabla}_x\phi^{\pm}|\right)=0.$$

Under the condition that the phase $\phi^{\pm}$ is regular, the bilinear form associated to the Hessian of the phase is symmetric, such that

$$\left(\overline{\overline{\nabla}}_x\left(\boldsymbol{\nabla}_x\phi^{\pm}\right).\boldsymbol{u}_0\right).\boldsymbol{\nabla}_x\phi^{\pm}=\left(\overline{\overline{\nabla}}_x\left(\boldsymbol{\nabla}_x\phi^{\pm}\right).\boldsymbol{\nabla}_x\phi^{\pm}\right).\boldsymbol{u}_0.$$

It remains only to note that $\partial_\mu\left(\dfrac{1}{|\boldsymbol{\nabla}_x\phi^{\pm}|}\right)=-\dfrac{\partial_\mu\left(\boldsymbol{\nabla}_x\phi^{\pm}\right).\boldsymbol{\nabla}_x\phi^{\pm}}{|\boldsymbol{\nabla}_x\phi^{\pm}|^3}$, which leads to the following equation

$$-|\boldsymbol{\nabla}_x\phi^{\pm}|\partial_t\left(\frac{1}{|\boldsymbol{\nabla}_x\phi^{\pm}|}\right)-|\boldsymbol{\nabla}_x\phi^{\pm}|\boldsymbol{u}_0.\boldsymbol{\nabla}_x\left(\frac{1}{|\boldsymbol{\nabla}_x\phi^{\pm}|}\right)+\frac{1}{|\boldsymbol{\nabla}_x\phi^{\pm}|^2}\boldsymbol{\nabla}_x\phi^{\pm}.\left(\boldsymbol{\nabla}_x\phi^{\pm}\overline{\otimes}\overline{\overline{\nabla}}_x\boldsymbol{u}_0\right)$$
$$\pm\frac{1}{|\boldsymbol{\nabla}_x\phi^{\pm}|}\boldsymbol{\nabla}_x\phi^{\pm}.\boldsymbol{\nabla}_x c_0\mp c_0\boldsymbol{\nabla}_x\phi^{\pm}.\boldsymbol{\nabla}_x\left(\frac{1}{|\boldsymbol{\nabla}_x\phi^{\pm}|}\right)=0,$$

which can be written as

$$\partial_t\left(\frac{1}{|\boldsymbol{\nabla}_x\phi^{\pm}|}\right)+\underbrace{\left(\boldsymbol{u}_0\pm c_0\frac{\boldsymbol{\nabla}_x\phi^{\pm}}{|\boldsymbol{\nabla}_x\phi^{\pm}|}\right)}_{\boldsymbol{v}_g^{\pm}}.\boldsymbol{\nabla}_x\left(\frac{1}{|\boldsymbol{\nabla}_x\phi^{\pm}|}\right)$$
$$=\frac{1}{|\boldsymbol{\nabla}_x\phi^{\pm}|^3}\boldsymbol{\nabla}_x\phi^{\pm}.\left(\boldsymbol{\nabla}_x\phi^{\pm}\overline{\otimes}\overline{\overline{\nabla}}_x\boldsymbol{u}_0\right)\pm\frac{1}{|\boldsymbol{\nabla}_x\phi^{\pm}|^2}\boldsymbol{\nabla}_x\phi^{\pm}.\boldsymbol{\nabla}_x c_0.$$

□

Appendix B: Source term of the equation (19)

Recall that W_0 denote the mean flow profile. We begin by demonstrating that

$$<\boldsymbol{e}_{{}^t\Pi^{\pm}},W_0>=\frac{\rho_0}{2},\tag{48}$$

and

$$<\boldsymbol{e}_{{}^t\Pi^{\pm}},A_iW_0>=\frac{\rho_0 v_i}{2}.\tag{49}$$

First observe that the vector W_0 can be decomposed as

$$W_0=\rho_0\boldsymbol{e}_{\Pi^{\pm}}-\rho_0c_0\mathcal{V}^{\pm}\qquad\text{where }\mathcal{V}^{\pm}=\begin{pmatrix}0\\ \boldsymbol{w}_g^{\pm}\\ 0\end{pmatrix}.\tag{50}$$

We notice also that the vector $\boldsymbol{e}_{{}^t\Pi^{\pm}}$ is written as

$$\boldsymbol{e}_{{}^t\Pi^{\pm}}=\begin{pmatrix}\dfrac{1}{2}-\dfrac{1}{\rho_0}<\ell^{\pm},\bar{W}_0>\\ \\ \ell^{\pm}\end{pmatrix}\quad\text{with }\bar{W}_0=\begin{pmatrix}\rho_0\boldsymbol{u}_0\\ \\ \rho_0 s_0\end{pmatrix}\in\mathbb{R}^{d+1},\ \ell^{\pm}=\begin{pmatrix}\boldsymbol{w}_g^{\pm}\\ \\ \dfrac{c_0}{\gamma}\end{pmatrix}\in\mathbb{R}^{d+1}.$$

Trivially, we check $< \boldsymbol{e}_{t\Pi^\pm}, W_0 >= \dfrac{\rho_0}{2}$. To prove the other identity, we note that we have $< \boldsymbol{e}_{t\Pi^\pm}, A_i \boldsymbol{e}_{\Pi^\pm} >= v_i^\pm$, then using (50) we get:

$$< \boldsymbol{e}_{t\Pi^\pm}, A_i W_0 >= \rho_0 v_i^\pm - \rho_0 c_0 < \boldsymbol{e}_{t\Pi^\pm}, A_i \mathscr{V}^\pm > .$$

A direct calculation gives us

$$A_i \mathscr{V}^\pm = \begin{pmatrix} w_{g_i} \\ w_{g_i} \boldsymbol{u}_0 + u_{0_i} \boldsymbol{w}_g^\pm \\ s_0 w_{g_i} \end{pmatrix} = \frac{w_i}{\rho_0} W_0 + u_{0_i} \mathscr{V}^\pm.$$

Given that $|\boldsymbol{w}_g^\pm| = 1$ and using the first identity (48), we find

$$< \boldsymbol{e}_{t\Pi^\pm}, A_i \mathscr{V}^\pm >= \frac{w_{g_i}^\pm}{2} + \frac{u_{0_i}}{2c_0} = \frac{v_i^\pm}{2c_0}, \tag{51}$$

which finally gives

$$< \boldsymbol{e}_{t\Pi^\pm}, A_i W_0 >= \rho_0 v_i^\pm - \rho_0 c_0 \frac{v_i^\pm}{2c_0} = \frac{\rho_0 v_i^\pm}{2}.$$

Using the decomposition (50) and the identities (49)-(51), it follows that

$$< \boldsymbol{e}_{t\Pi^\pm}, \partial_i (A_i \boldsymbol{e}_{\Pi^\pm}) >= \frac{< \boldsymbol{e}_{t\Pi^\pm}, \partial_i (A_i W_0) >}{\rho_0} - \frac{v_i^\pm \partial_i \rho_0}{2\rho_0} + \frac{v_i^\pm \partial_i c_0}{2c_0} + c_0 < \boldsymbol{e}_{t\Pi^\pm}, \partial_i (A_i \mathscr{V}^\pm) > .$$

By the fact that the mean flow W_0 is solution of the Euler equations and according to the system (3), we verify that

$$\sum_{i=1}^{d} \partial_i (A_i W_0) = \begin{pmatrix} -\partial_t \rho_0 \\ -\boldsymbol{\nabla}_{\boldsymbol{x}} p_0 + \boldsymbol{\nabla}_{\boldsymbol{x}} (c_0^2 \rho_0) - \partial_t (\rho_0 \boldsymbol{u}_0) \\ -\partial_t (\rho_0 s_0) \end{pmatrix},$$

and using the perfect gas law, it follows

$$\sum_{i=1}^{d} \partial_i (A_i W_0) = \begin{pmatrix} -\partial_t \rho_0 \\ -p_0 \boldsymbol{\nabla}_{\boldsymbol{x}} s_0 + 2c_0 \rho_0 \boldsymbol{\nabla}_{\boldsymbol{x}} c_0 - \partial_t (\rho_0 \boldsymbol{u}_0) \\ -\partial_t (\rho_0 s_0) \end{pmatrix},$$

this brings us to

$$\sum_{i=1}^{d} < \boldsymbol{e}_{t\Pi^\pm}, \partial_i (A_i W_0) >= -\frac{p_0 \boldsymbol{w}_g^\pm . \boldsymbol{\nabla}_{\boldsymbol{x}} s_0}{2c_0} + \rho_0 \boldsymbol{w}_g^\pm . \boldsymbol{\nabla}_{\boldsymbol{x}} c_0 - \frac{\partial_t \rho_0}{2} - \frac{\rho_0 \boldsymbol{w}_g^\pm . \partial_t \boldsymbol{u}_0}{2c_0} - \frac{\rho_0 \partial_t s_0}{2\gamma}. \tag{52}$$

Always by (50), we have

$$\partial_i(A_i\mathscr{V}^\pm)=\partial_i\left(\frac{w^\pm_{g_i}}{\rho_0}\right)W_0+\frac{w^\pm_{g_i}}{\rho_0}\partial_i W_0+\partial_i u_{0_i}\mathscr{V}^\pm+u_{0_i}\partial_i\mathscr{V}^\pm.$$

By a direct calculation, we obtain

$$<\boldsymbol{e}_{\Pi^\pm},\partial_i W_0>=\frac{\partial_i\rho_0}{2}+\frac{\rho_0}{2c_0}\partial_i\boldsymbol{u}_0.\boldsymbol{w}^\pm_g+\frac{p_0\partial_i s_0}{2},$$

and thereafter

$$\sum_{i=1}^d\frac{w^\pm_{g_i}}{\rho_0}<\boldsymbol{e}_{\Pi^\pm},\partial_i W_0>=\frac{\boldsymbol{w}^\pm_g.\boldsymbol{\nabla}_{\boldsymbol{x}}\rho_0}{2\rho_0}+\frac{\boldsymbol{w}^\pm_g.\left(\boldsymbol{w}^\pm_g\bar{\otimes}\bar{\bar{\nabla}}_x\boldsymbol{u}_0\right)}{2c_0}+\frac{p_0\boldsymbol{w}^\pm_g.\boldsymbol{\nabla}_{\boldsymbol{x}}s_0}{2\rho_0}.\tag{53}$$

Using the fact that $|\boldsymbol{w}^\pm_g|=1$ and therefore $\boldsymbol{w}^\pm_g.\partial_i\boldsymbol{w}^\pm_g=0$, one gets

$$\sum_{i=1}^d\partial_i u_{0_i}<\boldsymbol{e}_{\Pi^\pm},\mathscr{V}^\pm>=\frac{\mathrm{div}\boldsymbol{u}_0}{2c_0}\quad\text{and}\quad\sum_{i=1}^d u_{0_i}<\boldsymbol{e}_{\Pi^\pm},\partial_i\mathscr{V}^\pm>=0.\tag{54}$$

Combining (48), (53), and (54), we find

$$\sum_{i=1}^d<\boldsymbol{e}_{\Pi^\pm},\partial_i(A_i\mathscr{V}^\pm)>=\frac{\mathrm{div}\boldsymbol{v}^\pm_g}{2c_0}+\frac{\boldsymbol{w}^\pm_g.\left(\boldsymbol{w}^\pm_g\bar{\otimes}\bar{\bar{\nabla}}_x\boldsymbol{u}_0\right)}{2c_0}+\frac{p_0\boldsymbol{w}^\pm_g.\boldsymbol{\nabla}_{\boldsymbol{x}}s_0}{2\rho_0}-\frac{\boldsymbol{w}^\pm_g.\boldsymbol{\nabla}_{\boldsymbol{x}}c_0}{2c_0}.\tag{55}$$

Combining (52)and (55), we deduce

$$\begin{aligned}\sum_{i=1}^d<\boldsymbol{e}_{\Pi^\pm},\partial_i(A_i\boldsymbol{e}_{\Pi^\pm})>=&\frac{\mathrm{div}\boldsymbol{v}^\pm_g}{2}-\frac{\boldsymbol{v}^\pm_g.\boldsymbol{\nabla}_{\boldsymbol{x}}\rho_0}{2\rho_0}+\frac{\boldsymbol{v}^\pm_g.\boldsymbol{\nabla}_{\boldsymbol{x}}c_0}{2c_0}+\frac{\boldsymbol{w}^\pm_g.\left(\boldsymbol{w}^\pm_g\bar{\otimes}\bar{\bar{\nabla}}_x\boldsymbol{u}_0\right)}{2}\\&+\frac{\boldsymbol{w}^\pm_g.\boldsymbol{\nabla}_{\boldsymbol{x}}c_0}{2}+-\frac{\partial_t\rho_0}{2\rho_0}-\frac{\boldsymbol{w}^\pm_g.\partial_t\boldsymbol{u}_0}{2c_0}-\frac{\partial_t s_0}{2\gamma},\end{aligned}$$

which shows the desired result.

Appendix C: Reduced geometric spreading

Proposition C.1. *If the mean flow is independent of the time, and if the solution of the eikonal equation is written as $\phi(t,\boldsymbol{x})=\phi_1(t)+\phi_2(\boldsymbol{x})$ or $\phi(t,\boldsymbol{x})=\tilde{\phi}_1(t)\phi_2(\boldsymbol{x})$ where $\tilde{\phi}_1$ is a strictly positive function, then the geometrical spreading is reduced to:*

$$J(s,\boldsymbol{\beta})=-|\partial_s\boldsymbol{x}(s,\boldsymbol{\alpha})\ \partial_{\boldsymbol{\alpha}}\boldsymbol{x}(s,\boldsymbol{\alpha})|,$$

where $\boldsymbol{\beta}\equiv(t_0,\boldsymbol{\alpha})\in\mathbb{R}\times\mathbb{R}^{d-1}$ is a parameterization of the incident surface Σ_{inc}.

Proof. In these cases, the equation on the ray field is written

$$\frac{\partial \boldsymbol{x}}{\partial s}(s,\boldsymbol{\beta}) = \boldsymbol{u}_0(\boldsymbol{x}(s,\boldsymbol{\beta})) + c_0(\boldsymbol{x}(s,\boldsymbol{\beta}))\frac{\boldsymbol{\nabla}_{\boldsymbol{x}}\phi_2(\boldsymbol{x}(s,\boldsymbol{\beta}))}{\left|\boldsymbol{\nabla}_{\boldsymbol{x}}\phi_2(\boldsymbol{x}(s,\boldsymbol{\beta}))\right|},$$

that can be written also as

$$\frac{\partial \boldsymbol{x}}{\partial s}(s,\boldsymbol{\beta}) = \mathscr{F}(\boldsymbol{x}(s,\boldsymbol{\beta})). \tag{56}$$

By deriving the above equation with respect to t_0, it follows that

$$\frac{\partial}{\partial s}\left(\partial_{t_0}\boldsymbol{x}\right)(s,\boldsymbol{\beta}) = \nabla_{\boldsymbol{x}}\mathscr{F}\left(\boldsymbol{x}(s,\boldsymbol{\beta})\right).\partial_{t_0}\boldsymbol{x}(s,\boldsymbol{\beta}).$$

Given that $\boldsymbol{x}(0,\boldsymbol{\beta}) = (\boldsymbol{\alpha},0)$, it ensues that $\partial_{t_0}\boldsymbol{x}(0,\boldsymbol{\beta}) = \mathbf{0}_d$. By uniqueness of the solution of the equation (56), we deduce that $\partial_{t_0}\boldsymbol{x}(s,\boldsymbol{\beta}) = \mathbf{0}_d$ for all s.

It remains to note that the geometrical spreading is expressed as the sum of two determinants:

$$J(s,\boldsymbol{\beta}) = \left|\partial_{t_0}\boldsymbol{x}(s,\boldsymbol{\beta})\ \ \partial_{\boldsymbol{\alpha}}\boldsymbol{x}(s,\boldsymbol{\beta})\right| - \left|\partial_s\boldsymbol{x}(s,\boldsymbol{\beta})\ \ \partial_{\boldsymbol{\alpha}}\boldsymbol{x}(s,\boldsymbol{\beta})\right|.$$

This completes the proof of Proposition. □

In this case the function U simplifies to

$$U(t,\boldsymbol{x}) = \begin{pmatrix} \partial_\alpha \boldsymbol{x}\left(\mathscr{S}_0(t,\boldsymbol{x}),\mathscr{Y}_0(t,\boldsymbol{x})\right) \\ \partial_\alpha \xi\left(\mathscr{S}_0(t,\boldsymbol{x}),\mathscr{Y}_0(t,\boldsymbol{x})\right) \end{pmatrix},$$

which is solution of the same transport equation (29), but where the second derivatives of the Hamiltonian $\mathscr{H}^{\pm}$ are replaced by those of the Hamiltonian $H^{\pm}$.

References

[1] G. Barles: Solutions de viscosité des équations de Hamilton-Jacobi. Springer, Berlin (1994)

[2] J.D. Benamou, O. Lafitte, R. Sentis, I. Solliec: A geometric optics method for high frequency electromagnetic fields computations near fold caustics Part I, J.Comp.Appl.Math., 156, 93-125 (2003). 21, 27

[3] J.D. Benamou, O. Lafitte, R. Sentis, I. Solliec: A geometric optics method for high frequency electromagnetic fields computations near fold caustics Part II, J.Comp.Appl.Math., 167, 91-134 (2004) 4, 21, 31, 51

[4] D. Bouche, F. Molinet: Méthodes asymptotiques en électromagntisme. Mathématiques et Applications (vol. 16), Springer-Verlag (1996) 4, 17, 51

[5] M. Bruneau: Manuel d'acoustique fondamentale. Hermes (1998) 3

[6] M.G. Crandall, P.L. Lions: Viscosity solutions of Hamilton-Jacobi equations, Trans. Amer. Math. Soc., 277, 1-42 (1983) 27

[7] M.G. Crandall, P.L. Lions: Two approximation solutions of Hamilton-Jacobi equations. Math.Comp, 43, 1-19 (1984)

[8] S. Duprey: Étude mathématique et numérique de la propagation acoustique dans un turboréacteur, Thèse de mathématique de l'université Henry-Poincaré Nancy1 (2006) 4, 21, 23

[9] B. Engquist, E. Fatemi, S. Osher: Numerical resolution of the high frequency asymptotic expansion of the scalar wave equation, J. Comp. Physics, 120, 145-155 (1995) 3

[10] B. Engquist, O. Runborg: Computational high frequency wave propagation, Acta Numerica, 12, 181-266 (2003)

[11] K.O. Friedrichs: Symmetric hyperbolic linear differential equations, Comm. Pure Appl.Math., 7, 345-392 (1954)

[12] K.O. Friedrichs, P. Lax: Boundary value problems for first order operators, Comm. Pure Appl.Math., 18, 355-388 (1965) 3

[13] F.G. Friedlander: The Wave equation on a curved space-time. Cambridge University Press (1975) 4, 6

[14] F.G. Friedlander, J.P. Keller: Asymptotic expansions of solutions of $(\triangle + k^2)u = 0$, Comm. Pure. Appl. Maths, 8 (3), 387-394 (1955) 7

[15] F.G. Friedlander: Sound Pulses. Cambridge University Press (1958)

[16] O. Guès: Développement asymptotique des solutions exactes des systèmes hyperboliques quasilinéaires, Asympt. Anal, 6, 241-269 (1993) 8

[17] A.Harten, B.Engquiqst, S.Osher, S.Chakravarthy, Uniformly high order accurate essentially non oscilattory schemes III, J.Comput.Phys, 71, 231-303 (1987)

[18] L. Hörmander: The analysis of linear partial differential operators I. Springer-Verlag (1985) 3

[19] L. Hörmander: The analysis of linear partial differential operators Ⅱ. Springer-Verlag (1985) 35

[20] J.L. Joly, G. Métivier, J. Rauch, Formal and rigorous nonlinear high frequency hyperbolic waves, Pitman Research Notes in Math, 253, 121-143 (1992) 10, 11

[21] J.L. Joly, G. Métivier, J. Rauch: Coherent and focusing multidimensional nonlinear geometric optics, Ann. Scient. Ec .Norm. Sup., 4eme série, tome 28, 51-113 (1995) 8

[22] J.B. Keller, S.I. Rubinow: Asymptotic solution of eigenvalue problems, Annals of Physics, 9, 24-75 (1960) 3

[23] J.B. Keller: A geometrical theory of diffraction. In Calculus of variations and its applications, Vol 8.McGraw-Hill, New-York (1958) 3

[24] O. Lafitte, Y. Noumir, J. Rauch: Conservation laws and fold caustics in the high frequency regime, To appear 3, 8

[25] L.D. LANDAU, E.M. LIPSCHITZ: Fluid Mechanics. Pergamon Press, Oxford (1987) 3

[26] P.D. Lax: Asymptotic solutions of oscillatory initial value problems, Duke Math Journal 24, 627-646 (1957) 16, 51, 52

[27] P.D. Lax: Hyperbolic Partial Differential Equations. Courant lecture notes 14, AMS (2006) 4

[28] G. Legendre: Rayonnement acoustique dans un fluide en écoulement: Analyse mathématique et numérique de l'équation de Galbrun, thèse Université Pierre et Marie Curie (2003) 4, 8

[29] D. Ludwig: Uniform asymptotic expansions at a caustic, Comm.Pure.Appl.Math, 19, 215-250 (1960)

[30] D. Ludwig: Exact and asymptotic solutions of the Cauchy problem, Comm.Pure.Appl.Math, 14, 113-124 (1961) 3

[31] A. Majda, S. Osher: Initial-boundary value problems for hyperbolic equations with uniformly characteristic boundary, Comm. Pure Appl. Math., 28(5), 607-675 (1975)

[32] Y. Noumir: Une analyse haute fréquence des équations de l'aéroacoustique: étude mathématique et simulations numériques, thèse université Paris13 (2010) 8

[33] Y. Noumir and O. Lafitte, High frequency and numerical Eulerian methods for aeroacoustic problems, Journal of Computational and Applied Mathematics, Volume 204 Issue 2, 537-548 (2007)

[34] S. Osher, C.W. Shu: High-order essentially nonoscillatory schemes for Hamilton-Jacobi equations, SIAM J.Numer.Anal, Vol 28 (4), 907-922 (1991) 26, 52

[35] S. Piperno, M. Bernacki: A dissipation-free time-domain Discontinuous Galerkin method applied to three dimensional linearized Euler equations around a steady-state non-uniform inviscid flow, J. Computational Acoustics, vol. 14 (4), 445-467 (2006) 26

[36] J. Rauch: Lectures on Geometric Optics, in Nonlinear Wave Phenomena. eds. L. Caffarelli and W. E., IAS/Park City Math Series Vol. 5 (1998) 21, 23, 26, 35

[37] E. Rouy, A. Tourin: A viscosity solution approach to shape-from-shading, SIAM J.Numer.Anal., 29, 867-884 (1998) 3

[38] C.W. Shu: Essentially Non-Oscillatory and Weighted Essentially Non-Oscillatory Schemes for Hyperbolic Conservation Laws, NASA/CR-97-206253 ICASE Report No. 97-65A (1997) 4, 7, 14

[39] I. Solliec: Optique géométrique eulérienne et calcul d'énergie électromagnétique en présence de caustiques de type pli, Ph.D dissertation, Université Pierre et Marie Curie (2003) 4

[40] P. Souganidis, Approximation schemes for viscosity solutions of Hamilton-Jacobi equations, J. Diff. Eqns., 59, 1-43 (1985)

[41] M. Taylor: Partial Differential Equations, Basic Theory. Texts in Applied Math., 23, Springer-Verlag (1996)

[42] B. Van Leer: A second order sequel to Godunov's method, Journal of Computational Physics, 32, 101-136 (1979) 23

[43] J. Vidale: Finite-difference calculation of traveltimes, Bull. Seis. Soc. Am., 78, 2062-2076 (1988) 10